**Fermilab**

SYSTEM:



CCM



CVM



PLANT

TITLE: Director's Exception for CCM Vacuum Vessel

August 1, 1985

TO: Ken Stanfield, Research Division
FROM: *RW Fast*
Ron Fast, Cryogenics Department
SUBJECT: Director's Exception for CCM Cryostat

At the request of the Cryosafety Review Panel, we are seeking a Director's Exception for the CCM cryostat. John O'Meara, the Panel chairman, and I met with Dick Lundy on June 27, 1985 and told him that the helium vessel was not designed in accordance with chapter 14.1 of the Fermilab Safety Manual and that it was almost impossible to prepare the exceptional vessel engineering note called for in 14.1. He recommended that we postulate a failure of the helium vessel, calculate the resulting pressure in the vacuum vessel and test the vacuum vessel to 1.5 times this calculated pressure. This would adequately address the life safety issue, but would not guarantee no damage to the equipment following the postulated failure. We have now completed the calculation and the pressure test. The attached document summarizes the vessel nonconformance and records the calculations and test procedure/results.

RF/tg

cc: S. Stoy
J. O'Meara
A. McInturff
J. Misek
C. Bonham
R. Scherr
T. Kirk

PRESSURE VESSEL ENGINEERING NOTE
PER MANDATORY STANDARD SD37
(CHAPTER 14.1, LAB SAFETY MANUAL)

Prepared by: R.W. Fast

Preparation date: August 1, 1985

5.1 Description and Identification

Fill in the label information below:

This vessel conforms to engineering standard SD37

Vessel Title CCM Vacuum Vessel

Vessel Number RD 1089

Vessel Photo Number 83-482-6A

Relief Pressure 11.1 - 12.3 PSIG 25.8 - 27 PSIA

Working Temperature Range 100 °F -452 °F

Contents Vacuum liquid helium

Designer/Manufacturer Fermilab

Test Pressure (if tested at Fermi) 24 PSI, Hydraulic Pneumatic X

Acceptance Date: Jul 24 1985

Accepted as conforming to standard by K.C. Stanfield

of Division/Section Research Division

NOTE: Any subsequent changes in contents, pressures, temperatures, valving, etc., which affect the safety of this vessel shall require another review and test.

← Obtain from
Division/Section
Safety Officer

← Actual signature
required in this
space

Reviewed by: John E. O'Meara Date: 20 Aug 85

*Director's signature (or designee) if the vessel is for manned areas but doesn't conform to the requirements of the standard.

Richard A. Long Date: 8/21/85

Lab Property Number(s): Not applicable

Lab Location Code: NMS (obtain from Safety Officer)

Purpose of Vessel(s): To contain liquid helium in case of a rupture of the helium vessel.

Vessel Capacity/Size: 14100 liters

Normal Operating Pressure (OP) 0 PSIA

Worst-case relieving pressure 30 PSIA

Is the above enough to provide relief cracking pressure tolerance plus system uncertainty tolerance per M-9. YES

As an option, provide a photo of the entire vessel in the Appendix.

PRESSURE VESSEL ENGINEERING NOTE
PER MANDATORY STANDARD SD37
(CHAPTER 14.1, LAB SAFETY MANUAL)

Prepared by: R.W. Fast

Preparation date: August 1, 1985

5.1 Description and Identification

Fill in the label information below:

This vessel conforms to engineering standard SD37

Vessel Title CCM Vacuum Vessel

Vessel Number RD 1089

Vessel Photo Number 83-482-6A

Relief Pressure 11.1 - 12.3 PSIG 25.8 - 27 PSIA

Working Temperature Range 100 °F -452 °F

Contents Vacuum, liquid helium

Designer/Manufacturer Fermilab

Test Pressure (if tested at Fermi) 24 PSI, Hydraulic 24 PSI, Pneumatic X

Acceptance Date: Jul 24, 1985

Accepted as conforming to standard by _____

of Division/Section Research Division

NOTE: Any subsequent changes in contents, pressures, temperatures, valving, etc., which affect the safety of this vessel shall require another review and test.

← Obtain from
Division/Section
Safety Officer

← Actual signature
required in this
space

Reviewed by: _____ Date: _____

Director's signature (or designee) if the vessel is for manned areas but doesn't conform to the requirements of the standard.

_____ Date: _____

Lab Property Number(s): Not applicable

Lab Location Code: NMS (obtain from Safety Officer)

Purpose of Vessel(s): To contain liquid helium in case of a rupture of the helium vessel.

Vessel Capacity/Size: 14100 liters

Normal Operating Pressure (OP) 0 PSIA

Worst-case relieving pressure 30 PSIA

Is the above enough to provide relief cracking pressure tolerance plus system uncertainty tolerance per M-9. YES

As an option, provide a photo of the entire vessel in the Appendix.

List the numbers of all pertinent drawings and the location of the originals.
(Append copies).

<u>Drawing #</u>	<u>Location of Original</u>
5522.01-ME-28840C (1978-1979)	WH-11
5522.01-ME-28844F (1978-1980)	WH-11
5522.01-ME-28850B (1978-1980)	WH-11
5522.01-ME-28853A (1978)	WH-11

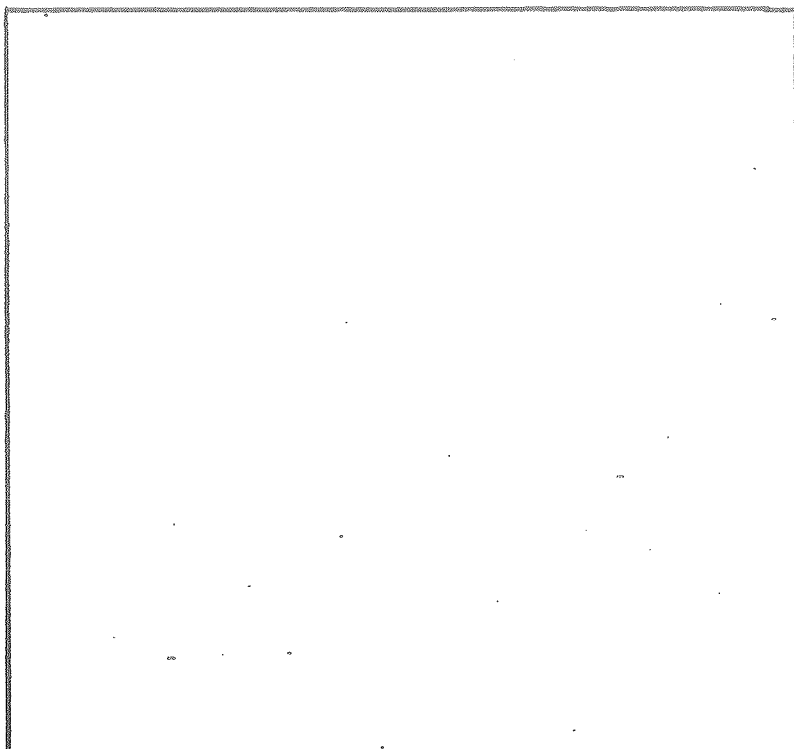
5.2 Design Verification

Does the vessel(s) have a U stamp? Yes _____ No X . If "Yes", fill out data below and skip page 3; if "No", fill out page 3 and skip this page.

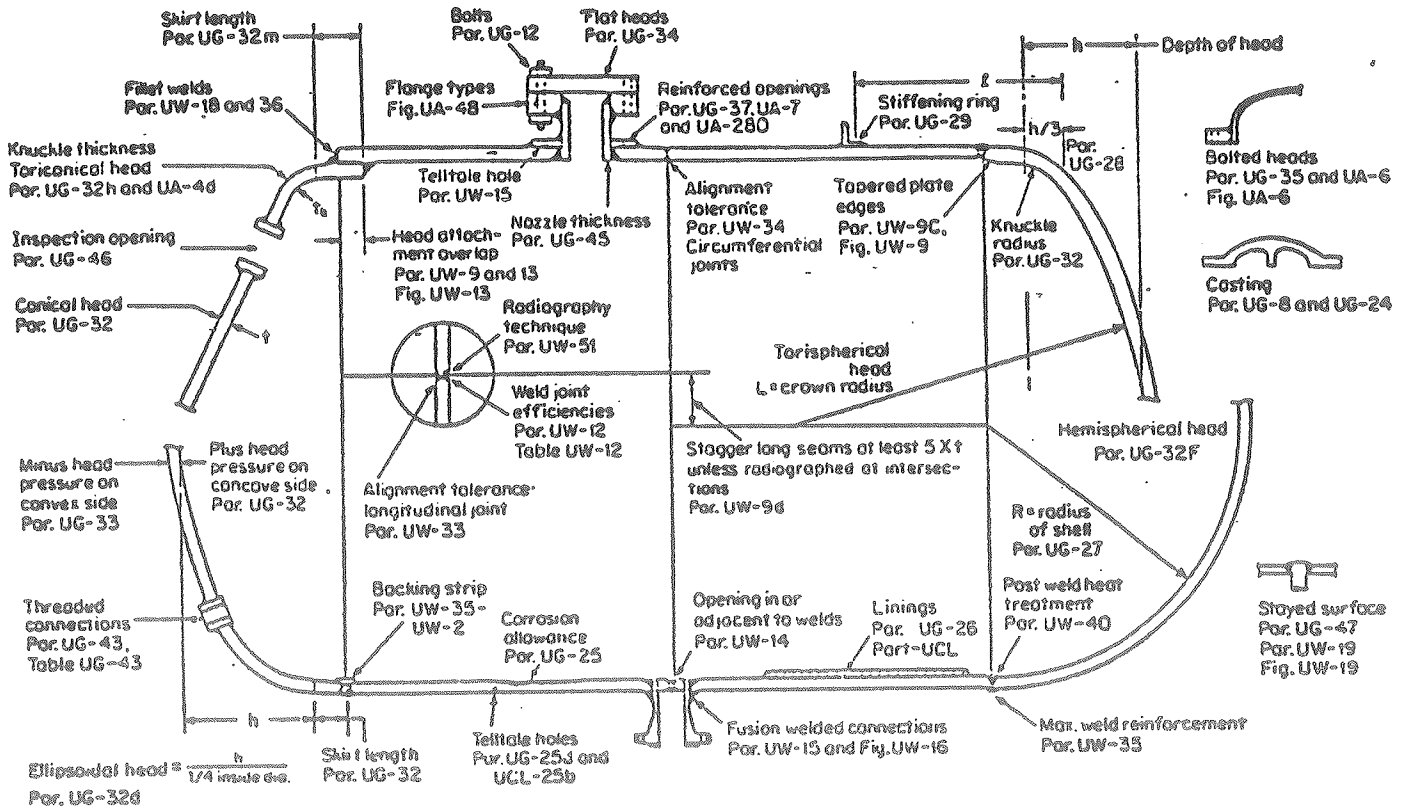
Staple photo of U stamp plate below.

Copy "U" label details to the side if photo is not clear or if copies are unreadable.

Copy data here:



On the sketch below, circle all applicable sections of the ASME code per Section VIII, Division I. List the results of all calculations. (Insert copies of calculations in the appendix).



Summary of ASME Code

CALCULATION RESULT
(Required thickness or stress level vs. actual thickness or calculated stress level)

<u>Item</u>	<u>Reference ASME Code Section</u>	<u>CALCULATION RESULT</u> (Required thickness or stress level vs. actual thickness or calculated stress level)
_____	_____	vs. _____
See Appendix A	_____	vs. _____
_____	_____	vs. _____
_____	_____	vs. _____
_____	_____	vs. _____

If this vessel is exceptional or had exceptional parts, list their details under 5.6. Yes X No _____

5.3 System Venting. Provide the system schematic in the Appendix, if the vessel safety is system sensitive. See system flow sheet, Appendix B.

Is it possible to isolate the relief valves by a valve from the vessel?

Yes _____ No X

If "Yes", the system must conform to M-5. Provide an explanation on the appended schematic. (An isolatable vessel, not conforming to M-5 violates the Standard.)

Is the relief cracking pressure set at or below the test pressure?

Yes X No _____ Actual setting _____ PSI
(A no response violates the Standard.)

Is the pressure drop of the relief system at maximum anticipated flow such that vessel pressure never rises above 2/3 of the test pressure?

Yes X No _____

Provide test or calculational proof in the Appendix.
(Non-conforming pressure rises violate the Standard.)

List of reliefs and settings:

<u>Manufacturer</u>	<u>Relief</u>	<u>Setting</u>	<u>Flow Rate</u>	<u>Size</u>
Fike -rupture disk	vacuum-PSV-636-V	11.1 psig	-	8"
Fike -rupture disk	vacuum-PSV-637-V	12.3 psig	-	4"
Fike -rupture disk	helium-PSV-632-H	11.7 psig	-	4"
Fike -rupture disk	helium-PSV-634-H	11.7 psig	-	4"
_____	_____	_____	_____	_____
_____	_____	_____	_____	_____

Is the relief device an ASME stamped device? Yes X No _____

5.4 Operating Procedure

Is an operating procedure necessary for the safe operation of this vessel?

Yes _____ No X. If "Yes", please append.

5.5 Welding Information

Has the vessel been fabricated in a Fermilab shop? Yes X No _____

If "Yes", append a copy of the welding shop statement of welder qualification and a copy of the Welding Procedure Specification (WPS) used to weld this vessel.

Not available

5.6 Exceptional, Existing, Used, and Non-Manned Area Vessels

Is this vessel or any-part thereof in the above categories? Yes X No _____

If "Yes", follow the Engineering Note requirements for documentation in free form below. Not possible, see Appendix A.

Appendix A: SUMMARY OF CCM CRYOSTAT SAFETY ANALYSIS

INTRODUCTION

The water-cooled copper coils on the Chicago Cyclotron Magnet (CCM) were replaced with a pair of superconducting coils as part of a Fermilab effort to conserve electrical power. After a two-year construction period the first, cryogenic test of the new coils, off of the iron, was held in the Meson Detector Building in the summer of 1980. The cryostats were then moved to the original Muon Laboratory (now called NWA) and tested to full current in February, 1981. Subsequently the magnet ran for two experimental running periods, 1981 and 1982. In the summer of 1983 the cryostats were demounted from the steel yoke. The steel was disassembled, moved to the site of the new Muon Laboratory and erected on a concrete foundation. The coils were stored outside in the Lab A parking lot during the 18-month construction period of the experimental hall (building NMS). The cryostats were reinstalled on the iron during the spring of 1985. At this writing (August 1 1985) the magnet is being prepared to operate for a test run of E-665 in August, 1985. A refrigerator-liquefier will be installed in NMS in 1986 to provide refrigeration for the CCM and the Cern Vertex Magnet (CVM), both of which will operate for a data run of E-665 in 1986.

Copies of the three published papers on the conversion of the CCM are given as Appendixes A1-3.

SUMMARY OF VESSEL DESIGN

The two superconducting coils are identical and are housed in identical helium coil chambers. A 2000-L helium reservoir is attached immediately above the upper coil chamber. For this reason the upper vacuum vessel, annular in shape, is larger in minor radius than the lower. The cryostat has eight major components: (1) upper helium vessel, (2) lower helium vessel, (3) upper nitrogen shield, (4) lower nitrogen shield, (5) upper vacuum vessel, (6) lower vacuum vessel, (7) chimney, and (8) the 24-column support system. The major portion of the design of the cryostat was completed by June, 1978.

Chapter 14.1 of the Fermilab Safety Manual, which establishes design and fabrication standards for room temperature pressure vessels, was initially implemented as Fermilab policy in 1981. It basically requires that such vessels be designed and fabricated in accordance with the ASME Pressure Vessel Code. Although 14.1 specifically exempts cryogenic vessels from this requirement, it has nevertheless been used as accepted practice in lieu of a standard for cryovessels. 14.1 also specifically exempts vacuum vessels from the Code requirements. However most dewar vacuum vessels at Fermilab have been designed in accordance with the Code for an external pressure differential of 7.5 psi.

Neither the helium vessel nor the vacuum vessel of the CCM was designed or fabricated in accordance with the Code. Sound engineering practice was used but Engineering Notes of the style required by 14.1 were not written at the time. It is almost impossible to cite every Code deficiency for the two vessels, but in general they fall into the following categories:

1. Allowable stresses: The allowable stress used in the design is somewhat higher than that specified in the Code. Specifically the designers took advantage of the higher strength of 304 stainless steel at cryogenic temperature, which is not permitted by the Code for that material.
2. Welding: Types of welds not permitted by the Code were used in several places on both vessels. Some of the weld reinforcements may also not be per Code. The assembly welding of the vessels was done by welders who were not Code certified. The weld procedures used were not specified and documented to Code requirements.
3. Materials control: The vessel subassemblies were fabricated by local shops which did not maintain the material inventory control required by the Code. Stainless steel is universally known to be sufficiently ductile at 4.2 K, so the designers did not require Charpy impact tests although the Code requires these tests be done for all materials used below -425°F .
4. Testing: The combined upper and lower helium vessel was pressure tested to a few psi prior to the 1980 cryogenic test. The vacuum vessel was leak checked using "Snoop" at an internal pressure of a few psig but, prior to the present tests, had not been formally "hydrostated".

ANALYSIS AND TESTING

Our assessment of the helium vessel is that since it was neither designed nor fabricated to the Code, the safety factor to rupture is probably less than that provided by a Coded vessel, which would be at least five. We have accordingly postulated a catastrophic rupture of the helium vessel and have addressed the life safety issue. We calculated the pressure to be expected in the vacuum vessel from this postulate using worst-case assumptions. We then tested the vacuum vessel to a pressure greater than this and found the stress intensities in the vacuum vessel to be less than would be permitted if the design had been done in accordance with the Code or FSM 14.1.

Sizing of Vacuum Vessel Relief System

The vacuum vessel is protected by two relief devices: a 4-IPS in-line Fike rupture disk on the lower vessel and an 8-IPS in-line disk on the upper vessel. The discharge lines from the disks tee into a 12-IPS, Sch 10 stainless steel vent line that leads out-of-doors. The helium system is relieved through two, 4-IPS Fike rupture disks into a second 12-IPS, Sch 10 stainless vent line leading out-of-doors. The pressure drop (rise) in this relief system has been calculated under what we feel is a worst-case failure, that of a sudden and complete rupture of the helium vessel which dumps 2000-L of liquid helium into the vacuum space. The result of this calculation, found in Appendix A4, is a vessel pressure of 15.3 psig.

Testing of Vacuum Vessel

The vacuum vessel was pneumatically tested to 1.57 times the pressure calculated above or 24 psig. A description of the test, the test procedure and the test result are given in Appendix A5. Strain gauges, placed at locations thought to be in high stress areas measured a stress intensity less than 8000 psi at the test pressure. None of the strain gauges showed a permanent set when the pressure was reduced to 0 psig.

CONCLUSION

Our calculation of the worst-case vacuum vessel pressure and the pressure test of the vacuum vessel give us confidence that the vacuum vessel and relief system will contain the helium following a rupture of the helium vessel. Both the upper and lower portions of the vacuum vessel and the interconnecting section of vacuum piping are shielded from the ambient environment by a 1/4" thick metal shroud.

We furthermore propose to implement the following restrictions on personnel access to the magnet area:

1. Once cooldown starts access into the fenced area at elevation 725 around the CCM will be restricted to magnet operators (Research Division Cryogenics Department staff and technicians) and E-665 experimenters and support personnel. Magnet operators will be on duty around the clock to enforce this restriction.
2. Access to the top of the magnet iron will be similarly restricted by use of a locked gate at the catwalk entrance (elevation 745) to the top of the iron. The key will be retained by the magnet operators at the magnet control rack.
3. The pit beneath the CCM will be classified as an ODH Class 1 area and an appropriate sign posted. The grating over the stairs leading into the pit will be locked and the key retained by the magnet operators.
4. Access to the magnet aperture when the helium vessel contains liquid helium will be restricted to staff and technicians of the Research Division Cryogenics Department and E-665 experimenters and support personnel. Access to the aperture will be prohibited when the magnet is energized.

A Cryogenic Engineering Conference Publication

Advances in Cryogenic Engineering

VOLUME 27

Edited by

R. W. Fast

Fermi National Accelerator Laboratory
Batavia, Illinois

PLENUM PRESS • NEW YORK and LONDON

26:
(1979).
(1979).
Sci.
Symp.
er,

THE SUPERCONDUCTING CHICAGO CYCLOTRON MAGNET

E. M. W. Leung, R. D. Kephart, A. S. Ito, and R. W. Fast

Fermi National Accelerator Laboratory
Batavia, Illinois*

INTRODUCTION

During the evening of February 21, 1981, the superconducting Chicago Cyclotron Magnet (CCM) reached a full field of 14.52 kG at a current of 900 A. This magnet, whose design, construction and cryogenic testing without iron have been reported earlier¹, became the world's second largest superconducting solenoid (in terms of radial dimensions) after the BEBC bubble chamber magnet at CERN. This paper describes the completed magnet test with iron (Fig. 1) and compares measurements to calculations. Performance of the 24 slider type four tube (three G-10 and one AISI 304 stainless steel) composite support columns, each capable of a collapse load of 1.33×10^6 N (3×10^5 lbs), is given in a separate paper². Essential magnet parameters are included in Table I.

STABILITY CONSIDERATIONS

To insure cryogenic stability in a pool boiling magnet, one might choose the Stekly parameter³, α , to be ≤ 1 . Another typical criterion is the maximum surface heat flux Y , from the conductor upon a complete transfer of current to the stabilizer. Keeping $Y \leq 0.3$ Wcm⁻² has been a conservative magnet design guideline for years. The authors feel that defining a parameter $\beta = I_{op} I_R$, is useful for the analysis of coil stability.

*Work supported by Universities Research Association, Inc. under contract with the U.S. Department of Energy.

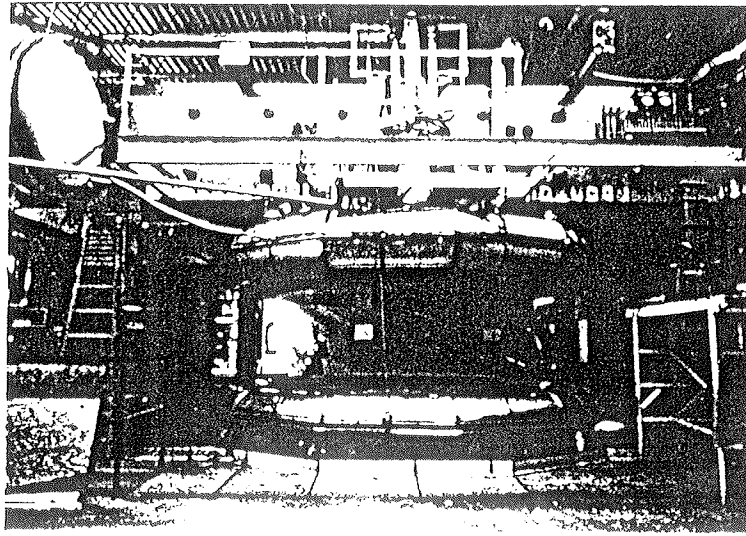


Fig. 1. A fish-eye view of the superconducting Chicago Cyclotron Magnet.

Table I. Magnet Parameters

Configuration:	Split solenoid (2 coils)
Winding I.D.:	5.19 m (204.4 in.)
Winding O.D.:	5.48 m (215.6 in.)
Cross section of each 100 turn coil:	142 mm x 117 mm (5.6 in. x 4.6 in.)
Spacing between coils:	1.85 m (73 in.)
Conductor specifics:	See Ref 1
Maximum test current:	900 A
Coil current density:	5415 A cm ⁻²
Conductor current density:	8611 A cm ⁻²
Stored energy at 900 A:	~ 26 MJ
Dump resistor:	0.2 Ω, center tap grounded
LHe refrigeration:	pool boiling, gravity fed, 2000 liter storage in magnet cryostat, intermittent transfer
Steady state LHe boil-off:	given in details later
Steady state LN ₂ boil-off:	200 L/day (calculated) 288 L/day (measured)
Magnetic field & forces:	Calculated using TRIM & GFUN ^{1,4,5,6}

Following Stekly,

$$I_R = I_C \sqrt{\alpha} \quad \alpha = \rho I_C^2 / h A f' p (T_C - T_b)$$

hence,

$$\beta = \sqrt{\alpha} (I_{op} / I_C)$$

= square root of the Stekly parameter \times fraction of the conductor short sample current at which the magnet is operated.

where

- ρ = electrical resistivity of the substrate of a conductor (including magnetic effect) at 4.2 K
- T_b = bath temperature
- T_C = critical temperature at I_C and B_m
- B_m = maximum magnetic field in the coil
- p = perimeter of conductor directly cooled by liquid helium
- $f'A$ = cross section of portion of conductor carrying current when in normal mode
- h = heat transfer coefficient to helium, depends on the construction details of the coil (e.g., width and orientation of cooling channels) ⁶
- α = Stekly parameter
- I_C = critical current of conductor at B_m and T_b
- I_R = full recovery current
- I_{op} = magnet operating current

The availability of cooling to the conductor is indicated by $\sqrt{\alpha}$ while I_{op} can be adjusted, such that $\beta < 1$. This approach is most useful when a compact coil has to be built. A choice of $0.9 < \beta < 0.95$ should be a good design criterion.

For the CCM coil, using a vertical channel correlation developed by M. Wilson ⁷, h is calculated to be $0.251 \text{ Wcm}^{-2}\text{K}^{-1}$, $T_C = 6.5 \text{ K}$, $B_m = 2.8 \text{ T}$, $I_C = 2500 \text{ A}$ (measured), $T_b = 4.2 \text{ K}$, $\rho = 2.68 \times 10^{-8} \text{ } \mu\text{cm}$, $f' = 0.74$, $p = 0.548 \text{ cm}$, $A = 0.1045 \text{ cm}^2$. Substituting into expressions given above, we get $\alpha = 6.85$ and $I_R = 955 \text{ A}$. Experimentally we have built a small test coil, to simulate the CCM coil cooling situation. It was found that the conductor operating at 900 A with a background field of 2.85 T will recover fully from an R-C heat pulse ($\tau = 30 \text{ ms}$) of 7.2 J over $\sim 1 \text{ cm}$ of conductor length. This experiment plus the detection of conductor motion during the initial charge up of CCM convinced us that the $\beta < 1$ criterion is a useful design aid. For CCM at a I_{op} of 900 A, β is 0.512 Wcm^{-2} .

An interesting plot of β vs. E , the magnetic store energy, for a number of pool boiling type super conducting solenoids, is shown in Fig. 2. For a given E , a high β represents a more aggressive design.

MAGNET TESTING AND COMPARISON TO CALCULATIONS

Cooldown, Charge Up and Field Measurements

We started the second LN_2 cooldown on February 2, 1981, at approximately the same rate as reported before.¹ By Feb. 8, both cryostats were filled with LN_2 . After allowing the whole system to sit in liquid nitrogen for 2 days and removing the remaining LN_2 by pressurizing the cryostats, we then blew gaseous helium through the system at low pressure (≤ 3 psig), to displace the residual and LN_2 and GN_2 and to subcool the coils to ~ 72 K. By adopting such a procedure, we required 1500 liters of LHe for further cooldown to 4.2 K instead of the 7000 liters estimated to be required for starting LHe cooldown at 90 K. This represents substantial monetary and time savings and hence a worthwhile procedure when one does not have a liquefier for cooldown. The steady state LHe boil-off without current dropped from 22.4 L/h 19 hours after first fill with LHe to 12.2 L/h 14 days later. It took a long time to reach equilibrium because of the extreme difficulty for the heat trapped in the intermediate AISI 304 column to escape, through long lengths of G-10, into the LHe temperature environment. We started the electrical testing by ramping up and down between 0 A and 200 A to make sure that all the interlocks and dump systems were working. On Feb. 21, we brought CCM up to 900 A in approximately 100 A steps.

The imbalanced voltage between the upper and the lower coils was continuously monitored as part of the quench detection

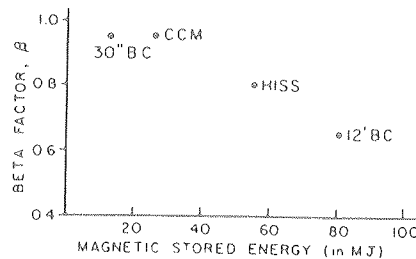


Fig. 2. β vs E for a few superconducting magnets of the same type Ref 8, 9, 10.

system. Prominent spikes of the order of a few volts which disappeared (or were present at smaller magnitude) on subsequent runs were observed. These observations during the first two charges of the magnet up to 700 A are presented in Fig. 3.

It can be seen that there were many more voltage excursions in the first charge. Simple calculations indicate that they are consistent with conductor motion. Such disturbances can grow into quench if the magnet is operating above the full recovery current. Hence, it is important to observe the $\beta < 1$ criterion.

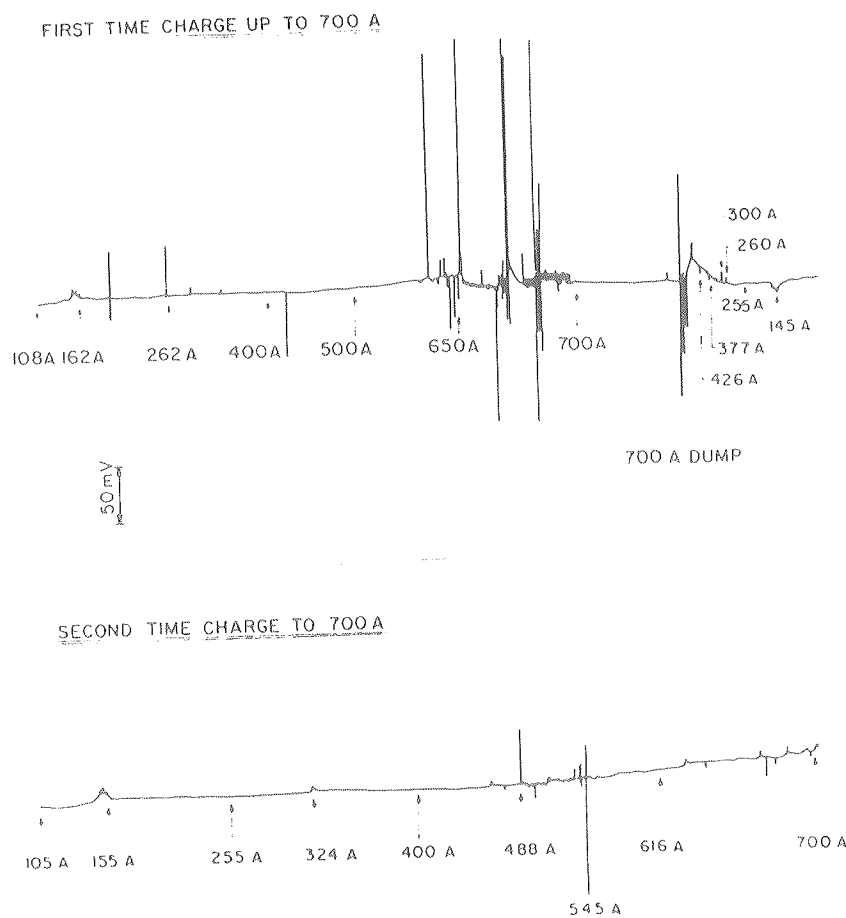


Fig. 3. Imbalanced voltages during charge.

Thermometry, LHe Consumption Rate and Cryogenic System Performance

The electrical resistance of the superconducting coils gives us two useful thermometers during cooldown, helping to generate graphs indicating the average cooldown rate of the magnet. Nine chromel-constantan thermocouples are located on the radiation shields, LN₂ intercepts of selected support columns and the power chimney. Cryogenic strain gages (MicroMeasurements WK-09-250BP-120) mounted on the AISI 304 tubes of 3 support columns provide the temperature by virtue of the apparent strain vs. temperature curves provided by the manufacturer. During the run, the average temperature of the LN₂ intercept on the support columns was ~ 97 K and that of the radiation shield ~ 87 K. Improvements to the LN₂ system to increase LN₂ flow will probably lower these temperatures and the LHe usage. With the present system, it is estimated that the equilibrium LHe consumption rate will be ~ 11 L/h (Fig. 4) with a T_{SS} = 62 K. Table II gives a breakdown of the heat leak in three different cases.

Table II. Heat Leak Into LHe System of CCM

	Best Measure- ments in Test without current	Anticipated steady state without current	Ideal case with Improved LN ₂ System
Temperatures defined in Fig. 4.	T _{RS} = 87.0 K T _{CI} = 97.0 K T _{SS} = 70.5 K	T _{RS} = 87 K T _{CI} = 97 K T _{SS} = 62 K	T _{RS} = 78 K T _{CI} = 80 K T _{SS} = 48 K
<u>Breakdown</u>			
Columns	4.7 W	3.9 W	2.7 W
Thermal Radiation	2.4 W	2.4 W	~ 1.5 W
Strain Gages	0.1 W	0.1 W	0.1 W
Chimney	0.3 W	0.3 W	0.3 W
Current Lead & Others	1.1 W	1.1 W	1.1 W
TOTAL	8.6 W (12.2 L/h)	7.8 W (11.1 L/h)	5.7 W (8.1 L/h)
With Current	10.0 W	implying that current leads do contribute additional heat load when in operation.	

where

1. A
...
...
...
...

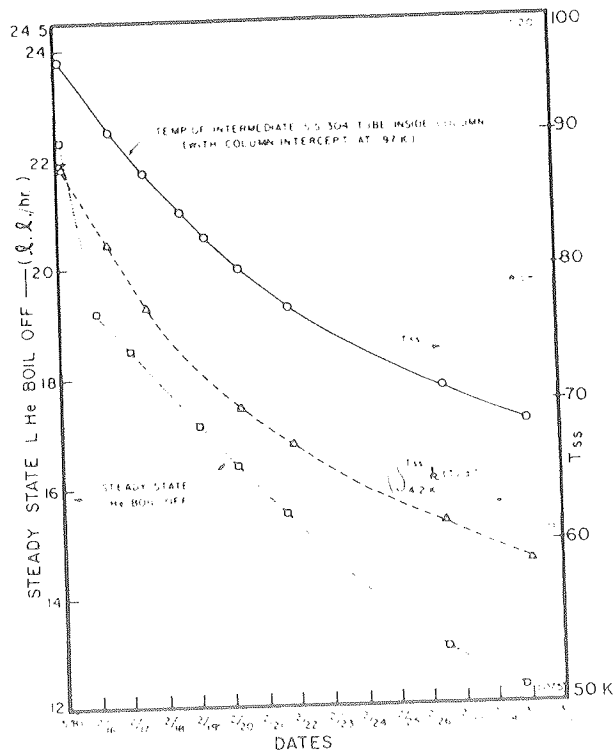


Fig. 4. Magnet LHe boil-off rate (without current), the temperature (T_{SS}) of the intermediate AISI 304 tube of the support column and the thermal conductivity integral of G-10 from T_{SS} to

$$4.2 \text{ K}, \int_{4.2}^{T_{SS}} k(T)dT, \text{ , against time.}$$

where T_{RS} = temperature of radiation shield
 T_{CI} = temperature of column liquid nitrogen intercept
 T_{SS} = temperature of intermediate stainless tube

CONCLUSION AND REMARKS

1. A very low heat leak pool boiling gravity fed superconducting magnet has been built. A new insulating method between 78 K and 4.2 K^{1,11}, which involves using an aluminum tape and 12 layers of NRC-2 superinsulation, is one of the contributing factors for low heat leak.
2. A beta factor has been introduced which should be useful in designing pool boiling type magnet, especially in the case

where the coil has to be very compact due to a limitation in space.

3. For a small additional heat leak, it is worthwhile to have ample instrumentation, to provide feedback for future if the magnet is a success and diagnostics if there are problems. For example, by having sufficient thermometry, we know that a lower LHe consumption rate can be achieved if the LN₂ is improved.
4. Substantial savings can be realized by conversion projects of this type. CCM will save 99% of the electrical power required to run the conventional magnet and ~ \$200,000 for each year of continuous operation.

REFERENCES

1. E.M.W. Leung, et.al., The superconducting Chicago cyclotron magnet—an old magnet with a new pair of energy efficient coils, IEEE Trans. on Magnetics, MAG-17 (1):199 (1981).
2. E.M.W. Leung, R.D. Kephart and C.P. Grozis, A Low Heat Leak Support Structural Member for the Superconducting Chicago Cyclotron Magnet, in "Advances in Cryogenic Engineering, Vol.27", Plenum Press, New York (1982).
3. Z.J.J. Stekly and J.L. Zar, Stable superconducting coils, IEEE Trans. on Nucl. Sci. NS-12:367 (1965).
4. R.J. Lari, Graphics, Time-Sharing Magnet Design Computer Programs at ANL, in "Proc. 5th Int. Conf. on Magnet Technology," Rome (1975), p. 244.
5. E.M.W. Leung, Magnetic Field Calculation of the Superconducting Version of the Chicago Cyclotron Magnet using GFUN-3D, Fermilab Technical Memorandum TM-759 (1978).
6. C.W. Trowbridge, Progress in Magnet Design by Computer, in "Proc. 4th Int. Conf. On Magnet Technology," Brookhaven (1972) p.555.
7. M.N. Wilson, Heat Transfer to Boiling Liquid Helium in Narrow Vertical Channels, in "Pure and Applied Cryogenics, Vol 6. Liquid Helium Technology," Pergamon Press, Oxford, England (1966).
8. Private communication, W.W. Craddock, Fermilab.
9. Private communication, R.C. Wolgast, Lawrence Berkeley Laboratory.
10. J.R. Purcell, The Superconducting Magnet System for the 12-Foot Bubble Chamber, Argonne National Laboratory Report, HEP-6813 (1968).
11. E.M.W. Leung, R.W. Fast, H.L. Hart, J.R. Heim, Technique for Reducing Radiation Heat Transfer Between 77 K and 4.2 K, in "Advances in Cryogenic Engineering, Vol. 25", Plenum Press, New York (1980) p. 489.

Ring
study
to the
coil
in the
by the
Detect
and m
mema
partic
minte
dents
cooled
on the

aw. 11

A Cryogenic Engineering Conference Publication

Advances in Cryogenic Engineering

VOLUME 27

Edited by

R. W. Fast

Fermi National Accelerator Laboratory
Batavia, Illinois

PLENUM PRESS · NEW YORK and LONDON

A LOW-HEAT-LEAK SUPPORT STRUCTURAL MEMBER FOR THE SUPERCONDUCTING CHICAGO CYCLOTRON MAGNET

E. M. W. Leung, R. D. Kephart, and C. P. Grozis

*Fermi National Accelerator Laboratory**
Batavia, Illinois

INTRODUCTION

The superconducting Chicago Cyclotron Magnet (CCM) at Fermilab has a pair of 5.33 m diameter split solenoid coils; the design, construction and testing of which had been reported earlier.^{1,2} The magnetic field and forces on these coils were calculated using the magnetic codes TRIM and GFUN-3D.³⁻⁵ Each coil is subjected to a very high axial attractive force (4.7×10^6 N) towards the iron yoke and this force increases at a rate of 6.34×10^6 N/m as the coil is displaced towards the yoke. In addition, the radial decentering force acting on each coil amounts to 7.88×10^5 N/m. The break-even point (the point at which LHe plus operation cost = electrical power cost) for the CCM conversion project is a liquid helium boil-off rate of ~ 40 L/h or ~ 28 W. As a result, to make the project cost effective requires the development of a support system that can react reliably and safely the aforementioned forces while at the same time achieving minimal heat leak into the 4.2 K environment.

We decided to react the vertical and de-centering force components with 12 slider-type composite support columns, equally spaced at 30° around the circumference of each coil. The major design goals for each of the 24 columns required were a collapse load of 1.33×10^6 N (300 KIPS) at operating condition, a heat load of < 150 mW into the LHe temperature environment, and the

*Operated by Universities Research Association, Inc. under contract with the U.S. Department of Energy.

ability to withstand the estimated decentering forces. In addition, the support system had to allow for the ~ 8 mm (on the radius) of radial differential thermal contraction that occurs during cooldown of the magnet.

DESIGN OF A SINGLE COLUMN

The primary structural support unit is a four-tube composite column. A short epoxy fiberglass (G-10) tube connects a slider (~ 300 K) to a LN_2 temperature heat sink. Between this heat intercept and the cryostat, there are three tubes, two G-10 and one AISI 304 stainless steel, connected together as shown in Fig. 1. A finished 4-tube assembly is shown in Fig. 2.

The stainless steel/G-10 transition joints are glued (Epon 815) and pinned such that they can take both tension and compression. It is also important for the flanges, (with the grooves accepting the ends of the G-10 tubes), at the ends of the intermediate stainless tube to be exactly parallel to each other. This facilitates assembly and reduces the possibility of the G-10 tubes breaking under compressive local end stresses. This was achieved by using electron beam welding which provided extremely small warpage (the flanges are parallel to each other to within 0.1 mm (0.004 inch) and high welding efficiency (measured to be over 98%). The large radial differential thermal contraction between the coil and the vacuum shell is taken care of by a slider mechanism designed into the column (Fig. 3). The sliding material is made of bronze impregnated Teflon, which has an extremely low coefficient of sliding friction (< 0.05). A thin-walled (0.25 mm) bellows closes the high vacuum circuit while permitting motion of the columns.

We considered using G-10CR instead of G-10 for the composite tubes. Although G-10CR has a higher strength than G-10, the strength/thermal conductivity ratio is about the same. We chose G-10 because of quicker delivery. We measured variations in the material properties of G-10 from different vendors and thus recommend careful testing procedures if G-10 is chosen for support structures. AISI 304 was chosen for the metallic tube because it lent itself better to welding when compared to either 6061-T6 aluminum or titanium.

PROTOTYPE TESTING

A minimum safety factor of three at normal operating condition was our goal. Room temperature mechanical testing was carried out and results extrapolated to lower operating temperatures since the low temperature strength characteristics of both G-10 and AISI 304 are fairly well known.⁶ The tube members are sized so that buckling is not possible.

ELECTRON
BEAM WELDING

Computer assisted

The
responding
tion.

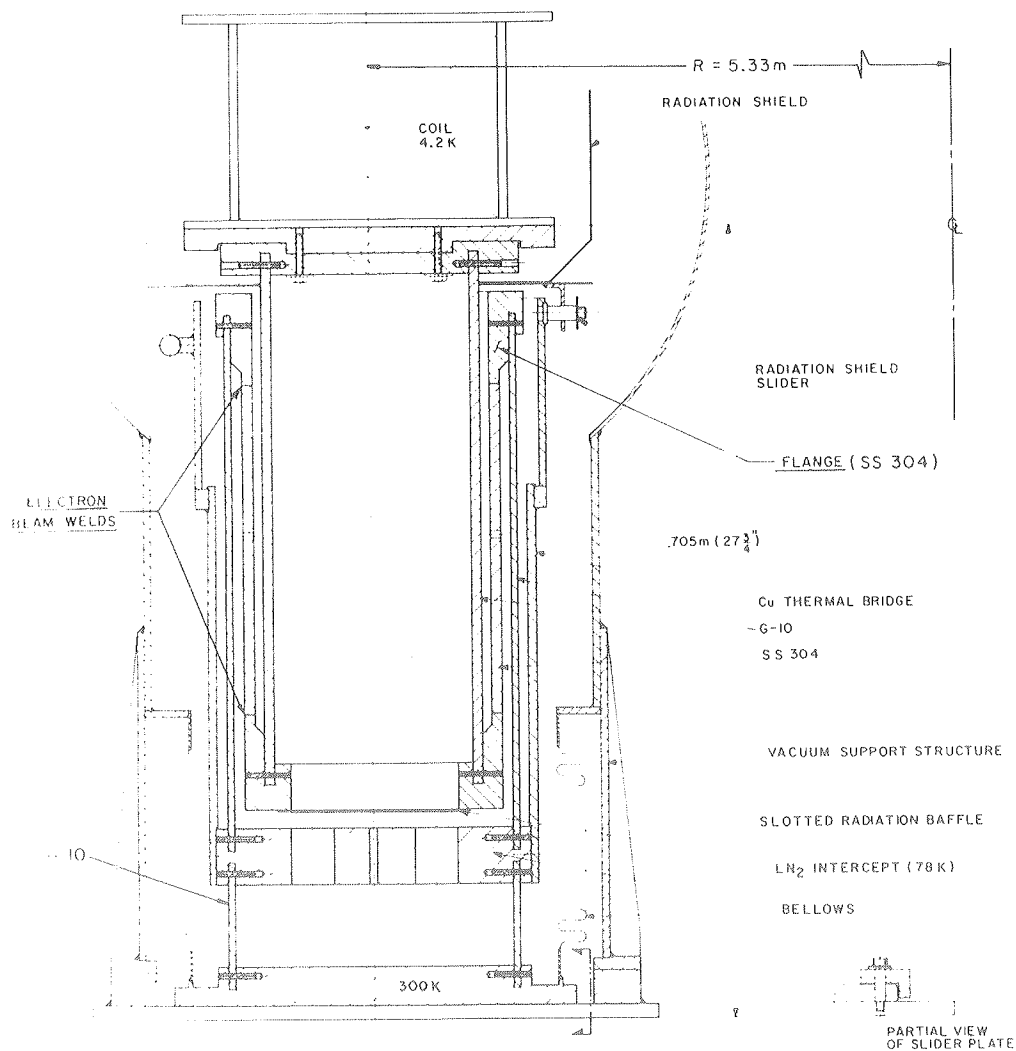


Fig. 1. Schematic of a Column.

Compression and Tension

The prototype was loaded to 8.9×10^5 N (200,000 lbs) corresponding to a load capacity of 1.78×10^6 N at operating condition.

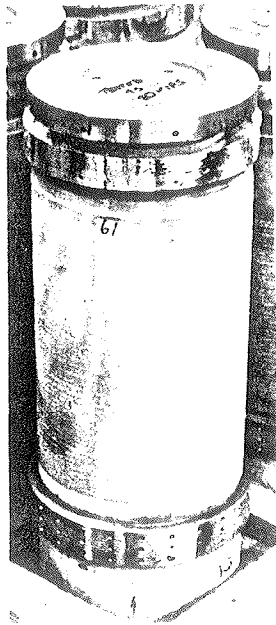


Fig. 2. A single column without slider.

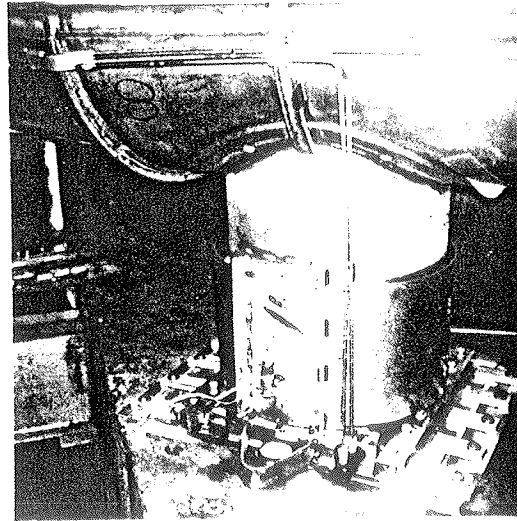


Fig. 3. An installed column on the lower coil.

Before the magnet is energized, the columns on the upper coil must support its weight. Each column has to hold 5.4×10^3 N in tension. The prototype was measured to have a yield strength of 1.82×10^4 N and calculated to have an ultimate tensile strength of 5.18×10^4 N.

Side Loading and Loading at an Angle

The lateral stiffness constant was calculated to be 2.6×10^{-6} m/N (4.5×10^{-5} in/lb) and measured to be 3.4×10^{-6} m/N (6.0×10^{-5} in/lb). Actual testing performed on the prototype showed yielding at a side load of 4504 N (1012.5 lbs). The radial decentering force for CCM is 7.9×10^5 N/m (4500 lb/in). If the coil were 2.54 cm from the magnetic center, the maximum side load that a column has to hold was calculated to be 2682 N (603 lbs). By careful surveying during the installation of the coils, we were able to locate the coils to within 6.4 mm (0.25 in) of the geometric center. Therefore, if the geometric and magnetic centers are the same, we can expect a safety factor of 6.7. The prototype was deliberately subjected to an excessive side load of 1.33×10^4 N (3000 lbs) and retested in compression. No significant degradation in performance (Fig. 4) was observed. We also loaded the prototype at an angle (gradient = 1/64) to simulate a situation

where a co
nented in F

Slider

The in
from the be
on a colum
action of m
5.

Proof Test I

Twenty
type testing
up to 6.7
test. They
three to 1,
given were
all the tube

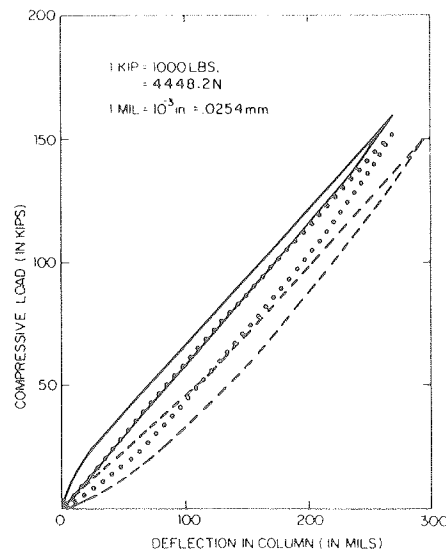


Fig. 4. A typical loading and unloading curve
 . . . before the prototype was yielded sideways
 ——— after the prototype was yielded sideways
 - - - after the prototype was yielded sideways and
 now loaded at an angle.

where a column is not well shimmed. The loading curve is presented in Fig. 4 also.

Slider

The frictional force from the slider and a retarding force from the bellows both contribute to a slider side loading effect on a column during cooldown. The system was optimized during a series of small tests. The final performance is presented in Fig. 5.

Proof Testing of All Columns Built

Twenty-six more support columns were built after the prototype testings. Each of them were subjected to a compression test up to 6.7×10^5 N (150,000 lbs) at room temperature and a creep test. They were all cycled up and down in the compression mode three to four times to make sure that the loading and unloading curves were repeatable. The creep test helps to make sure that all the tubes are correctly mated together.

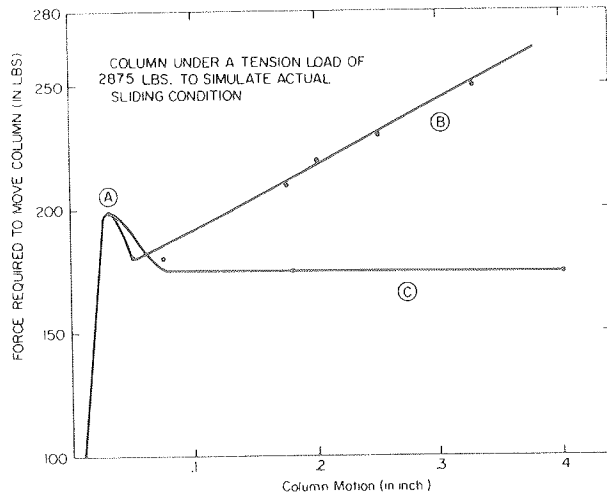


Fig. 5. Slider mechanism test

- (A) indicates that the coefficient of static friction is 0.070
 (B) indicates that the bellows lateral stiffness constant is $\Delta.82 \times 10^4$ N/m (275 lb/in)
 (C) indicates that the coefficient of sliding friction is 0.060.

System Performance During Magnet Testing

The three cryogenic strain gages on three separate intermediate stainless tubes and seven other gages calibrated to be used on G-10⁷, distributed over the various parts of different columns give an indication of the stress levels induced in the supports while the magnet is running (Table I).

A maximum stress of 142.8 MPa (20.7 Ksi) is found on the stainless intermediate tube close to the flange area. This is close to the calculated 129 MPa (18.7 Ksi). AISI 304 stainless steel in annealed form (assumed annealed close to weld) has a yield strength of 427.6 MPa (62 Ksi) at a temperature of 62 K, hence again a safety factor of three.

During cooldown and warmup, a linear potentiometer system with digital readout monitors the movement of the support columns relative to the coil cryostat, and a double-acting hydraulic system can be activated to push or pull on the base of the individual column to facilitate their motion.

Average
of 3
Average
of 3
Average
strain
(maxi

Mea
CCM ther
Instead
columns
stat via
our desi

We
high mec
Leak (-
low LHe
whole pro

1. E.M.W.
Ma
Co

2. E.M.W.
Ma
PI

3. R.J.
PI
Ro

4. E.M.W.
LI
AD
TB

5. C.W.
PI
CI

6. E.M.W.
Vol
2B

Table I. Column Stresses

	Measured Value	Calculated Value
Average stress on G-10 tube of 3 upper columns	58.5 MPa (8,487 psi)	56.2 MPa (8,150 psi)
Average stress on G-10 tube of 3 lower columns	48.3 MPa (7,000 psi)	56.2 MPa (8,150 psi)
Average stress on AISI 304 stainless steel tubes (maximum stress location)	137.9 MPa (20.0 Ksi)	129.0 MPa (18.7 Ksi)

Measurements during the actual operation indicated that the CCM thermal radiation shield was actually at a temperature of 87 K instead of the desired 78 K and that the LN₂ intercept of the columns was 97 K instead of 80 K. Estimated heat load into cryostat via each column amounts to 162.5 mW, which is within 10% of our design goal of 150 mW per column.

CONCLUSION

We have successfully built a support structure capable of high mechanical load (1.33×10^6 N in compression) and low heat leak (~ 150 mW). It contributed much to the achievement of the low LHe usage rate of CCM and therefore to the success of the whole project.

REFERENCES

1. E.M.W. Leung, et al., The Superconducting Chicago Cyclotron Magnet -- An Old Magnet with a New Pair of Energy Efficient Coils, IEEE Trans. on Magnetics 17:199 (1981).
2. E.M.W. Leung, et al., "The Superconducting Chicago Cyclotron Magnet," "Advances in Cryogenic Engineering, Vol 27," Plenum Press, New York (1982).
3. R.J. Lari, "Graphic, Time-Sharing Magnet Design Computer Programs at ANL," Proc. 5th Int. Conf. on Magnet Technology, Rome (1975), p. 244.
4. E.M.W. Leung, "Magnetic Field Calculation of the Superconducting Version of the Chicago Cyclotron Magnet using GFUN-3D," Fermi National Accelerator Laboratory Internal Report TM-759, January 1978.
5. C.W. Trowbridge, "Progress in Magnet Design by Computer," Proc. 4th Int. Conf. on Magnet Technology, Brookhaven (1972), p. 555.
6. F.R. Schwartzberg, et al., "Cryogenic Materials Data Handbook, Vol. 2," Air Force Materials Laboratory Report AFML-TDR-64-280 (1970).

7. S. Bonifas and E.M.W. Leung, "Measurement of Apparent Strain Curves of Two MicroMeasurements Strain Gauges Mounted on G-10," Fermi National Accelerator Laboratory Internal Report TM-987, August 1980.

HIGH

High
liquid hel
under whic
on the typ
each indiv
inductance
entire nam
magnetic m
field for t

Any c
reliable ca
maintain 0
ly 100 K.
contact att
with shunt
materials t
on the ord
small coeff

The co
bly, consist
11 cm long
multiple sta
connector,

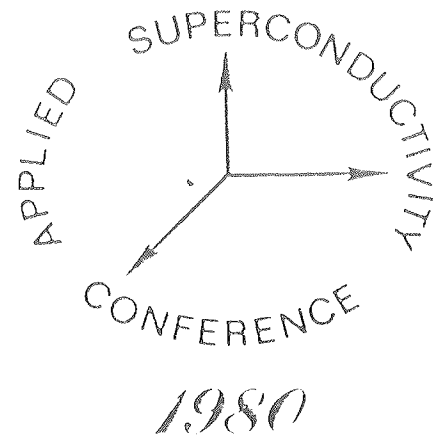
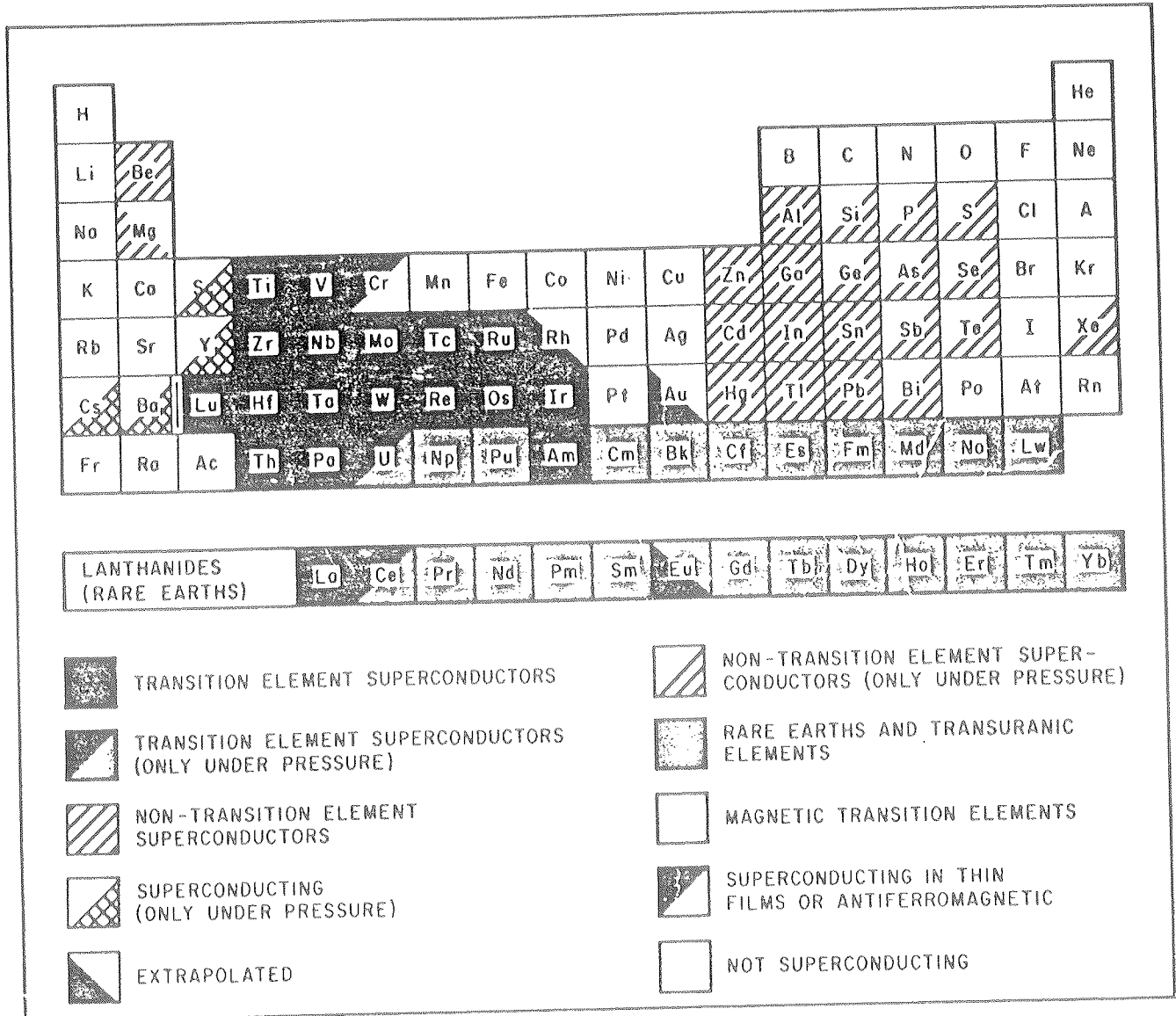
The app

MAGNETICS

JANUARY 1981 VOLUME MAG-17 NUMBER 1

(ISSN 0018-9464)

A PUBLICATION OF THE IEEE MAGNETICS SOCIETY



THE SUPERCONDUCTING CHICAGO CYCLOTRON MAGNET -
AN OLD MAGNET WITH A NEW PAIR OF ENERGY EFFICIENT COILS*

E.M.W. Leung, R.D. Kephart, R.W. Fast and J.R. Heim
Fermi National Accelerator Laboratory
P.O. Box 500
Batavia, Illinois 60510

Abstract

Significant electrical power can be saved by replacing existing water-cooled copper coils with superconducting ones. This paper describes a DOE-Fermilab energy conservation project in which a pair of superconducting tori 5.25 m in diameter have been constructed to replace the copper coils, built in 1949, of the 170-inch Chicago Cyclotron, now in use at Fermilab as an analysis magnet. The superconducting magnet, with a stored energy of 32.5 MJ, was fabricated in-house at Fermilab. Engineering concepts, design and optimization of the coil, support structure and cryogenic system are described. In particular, the major support, a composite column capable of a collapse load of $1.33 \times 10^6 \text{ N}$ and an expected heat leak of 120 mW will be described in detail. Practical problems encountered during the construction phase are discussed and test results presented.

Introduction

Fermi National Accelerator Laboratory has been active in the development and application of superconducting magnets since the founding of the laboratory. This frontier magnet technology is being applied to Doubler/Saver magnets, secondary beam transport magnets, experimental area analysis magnets and energy conservation coil conversion projects. The Chicago Cyclotron Magnet (CCM) Conversion Project belongs to the last category.

The Chicago Cyclotron magnet was constructed to provide the magnet field for a 450 MeV Cyclotron built at University of Chicago around 1949. After the Cyclotron was decommissioned, the magnet was transported to Fermilab in 1971 and reassembled for use as an analysis magnet in the FNAL Muon Laboratory where it resides currently. At full excitation, the existing copper coils consume 2.5 MW of electrical power. The savings brought about by having the coils superconducting can be formulated in terms of 1) more effective use of electrical power: that the 2.5 MW required to run the conventional CCM be used to power the Main Ring, hence producing higher intensity beams or cutting down the time duration for high energy physics experiments; or 2) monetary benefit: economic savings of up to \$200,000 can be generated by running the magnet superconducting, continuously for a year.

Design Philosophy & Requirements

To conserve and save is our primary objective. The amount of financial benefit brought about by a superconducting magnet is primarily determined by the heat transfer into the liquid helium environment. The heat leak, must, therefore, be reduced to a minimum without sacrificing reliability or cost. The break-even point (the point at which LHe plus operation cost = power cost) for the CCM project is a liquid helium boil-off rate of about 40 ℓ (liquid liters)/hour, or ~ 28 watts.

Magnet Field & Force Calculations

An important aspect of superconducting magnet design is magnetic field calculation. The more

accurately the directions and magnitude of the forces involved are known, the easier it is to design an optimized (with respect to heat leak) mechanical support system. The magnetostatic calculation was done using the axisymmetric form of TRIM¹ and the results checked with GFUN-3D.² A three-dimensional program like GFUN-3D is required for this case because of the asymmetry of the magnet iron (Fig. 1). Detailed results have been published as a Fermilab internal report.³ The magnet parameters are presented in Table I.

Table I
Magnet Parameters

Configuration:	Split solenoid (2 coils)
Winding inside diameter:	5.19 m (204.4 in.)
Radial thickness of winding:	14.2 cm (5.6 in.)
Vertical dimension of each coil:	11.7 cm (4.6 in.)
Spacing between coils:	1.85 m (73 in.)
Number of turns per coil:	1000
Operating current:	1000 A
Length of conductor per coil:	16.8 km
Current density in conductor:	9568 A/cm ²
Coil current density (average):	6017 A/cm ²
Central field:	1.5 T
Maximum field in coil:	2.85 T
Shelf inductance:	65 H
Stored energy:	32.5 MJ
Total vertical force towards iron for each coil ΣF_z :	$5.2 \times 10^6 \text{ N}$ ($1.17 \times 10^6 \text{ lbf}$)
Vertical force per unit length on each coil, F_v/ℓ :	$3.1 \times 10^5 \text{ N/m}$ (1777 lbf/in.)
Radial force per unit length on each coil, F_r/ℓ :	$2.7 \times 10^5 \text{ N/m}$ (1545 lbf/in.)
Radial decentering force, dF_r/dr :	$7.95 \times 10^5 \text{ N/m}$ (4500 lbf/in. displacement)
Nitrogen storage:	1850 liquid liters
Nitrogen use rate (measured):	300 liters/day (12.5 ℓ /hr)
Helium storage:	2000 liquid liters
Helium use rate (measured):	< 310 liters per day (< 13 ℓ /hr)

Coil Design and Construction

The CCM conductor used is a soldered cable with a Cu:SC:solder (70/30) ratio equal to 9.75:1:2.42. It consists of six 0.69 mm NbTi strands and eight 0.69 mm Cu strands soldered around a solid rectangular Cu core. The high copper to superconductor ratio ensures a safe margin for intrinsic stability. The coil structure (Fig. 2) is well defined and readily analyzed. Each coil was wound using a "wet lay-up" technique, with the insulating spacers wetted with epoxy and the whole coil then thermally cured to form a solid composite structure. The spacers serve a triple purpose: a) as load bearing members that transmit the electromagnetic

*Work sponsored by U.S. Department of Energy.

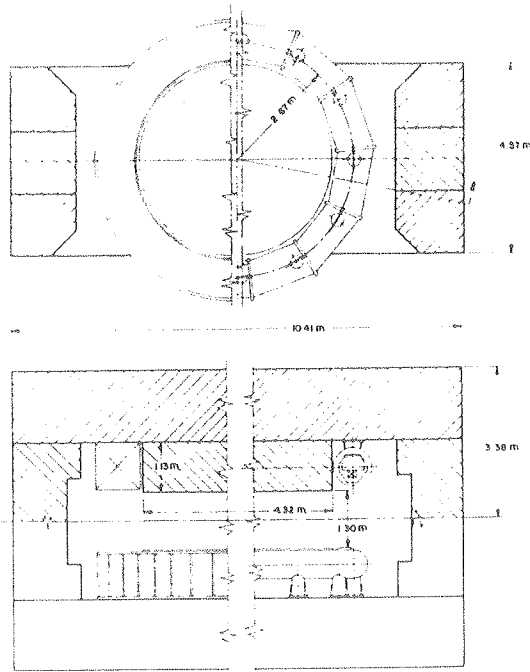


FIG. 1 A SECTION OF BOTH THE OLD AND NEW C.C.M

forces through the entire coil, b) as electrical insulators and c) to provide cooling channels through the coil. Individual conductors can then be treated analytically as a continuous beam on multiple supports. The radial force on each coil is carried by the helium vessel (SS 304) while the vertical force is reacted with 12 specially designed composite support columns, equally spaced at 30° around the coil (Fig. 1). Each coil is attached to the vessel wall with insulated mounting studs as shown in Fig. 2.

The primary support structure (Fig. 3) consists of a four-tube (three G-10 and one SS 304) composite column with a LN_2 temperature heat intercept and a slider mechanism to take care of the differential contraction between the coil and the vacuum shell. The sliding material is made of bronze impregnated Teflon, with an extremely low coefficient of sliding friction (< 0.05). A thin-walled bellows completes the high vacuum circuitry while permitting motion of the columns. Extensive testing had been carried out with a prototype. The column has a collapse load of 1.33×10^6 N in compression, tensile strength of 5.18×10^4 N and a design heat leak of less than 120 mW. The lateral stiffness constant was measured to be 3.43×10^{-4} mm/N (6.0×10^{-5} in/lbf). Under normal operating conditions (cryogenic temperature), each column sees a compressive load of 4.34×10^5 N. A safety factor of 3 is, therefore, provided. All 24 columns were proof-tested to a minimum of 6.65×10^5 N in compression at room temperature before installation.

Shell Construction & Cryogenic System

The helium shell is made from stainless steel 304 plates, assembled and welded to form a 12-sided polygonal annulus enclosing the coil. The lower shell is rectangular in cross section while that of the upper is larger and of strange shape (Fig. 4) to provide a 2000 l liquid helium storage space. The total amount of liquid helium in the magnet is about 3000 liters.

The LN_2 temperature radiation shield is made of 0.8 mm copper sheets fabricated to the correct shapes

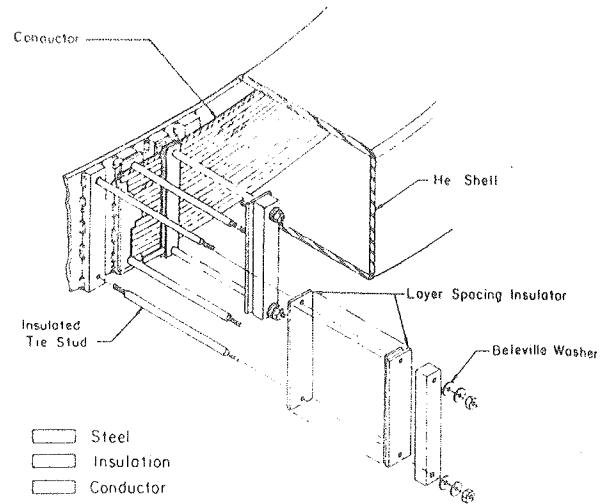


FIG. 2 COIL STRUCTURE

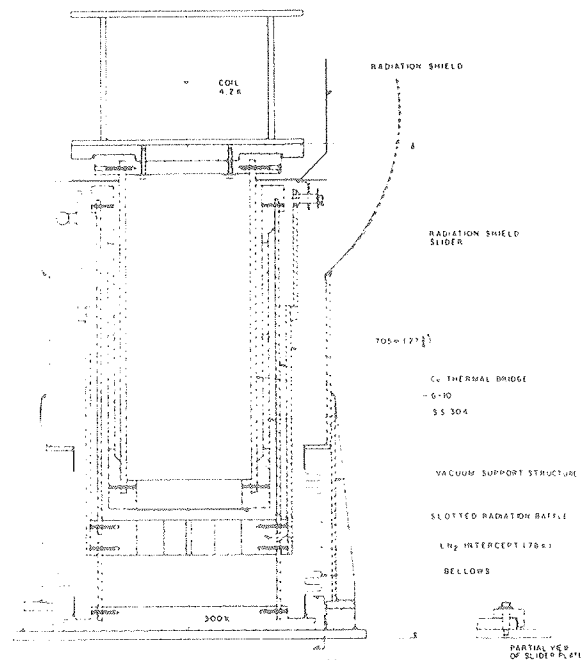


FIG. 3 COLUMN ASSEMBLY

and assembled with clips and self-taping machine screws. The thermal bridge (Figs. 3 and 4) of the columns provide mounting studs for the radiation shield to slide in and out on as the magnet is cooled down or warmed up.

The LN_2 system for CCM is a gravity-feed system (Fig. 5). It consists of an external 500 gal. (1850 liters) storage dewar, which supplies liquid to both the radiation shield and the intercepts on the columns, through cooling tubes that are attached to the Cu shield with specially designed flexible copper clips and rigidly attached to the thermal bridge of the columns via a mechanical arrangement. Indium is used in the latter to reduce thermal contact resistance. In all cases, the tubes slope upwards towards the top of the magnet.

The helium system, shown in Fig. 6, is also gravity fed. The vacuum shell is fabricated out of 3.175 mm (1/8") stainless steel (304) skin strengthened with ribs and cross bars.

Thermal Insulation

Radiation heat transfer in general contributes

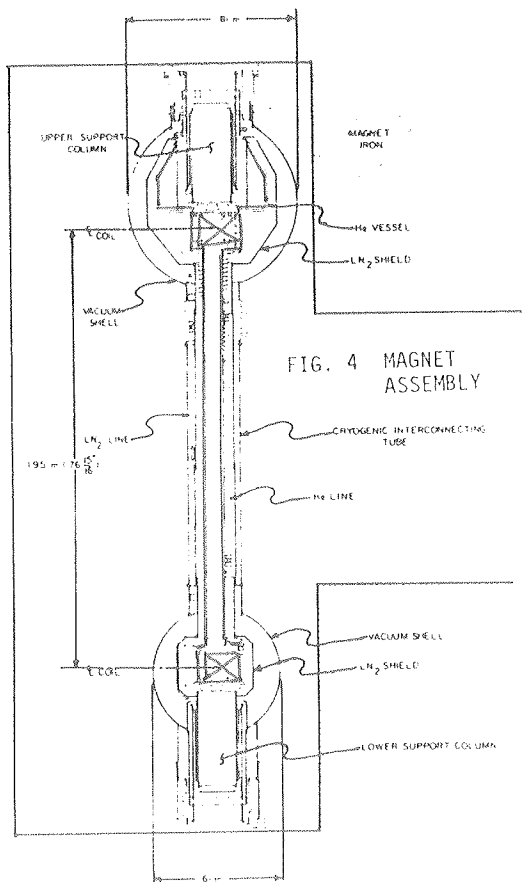


FIG. 4 MAGNET ASSEMBLY

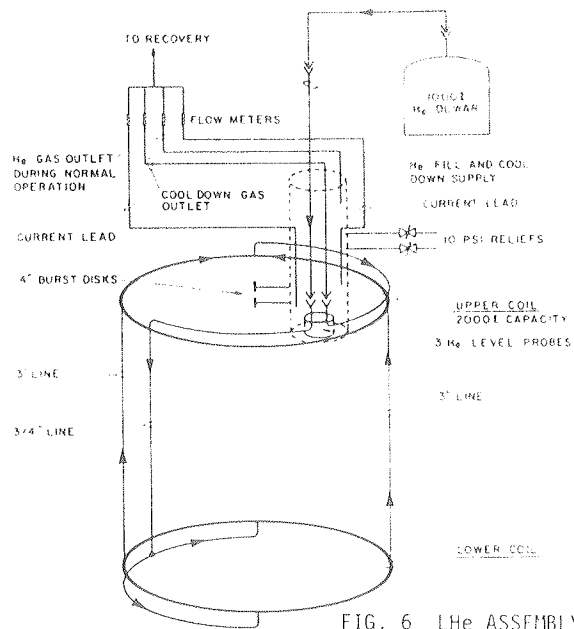


FIG. 6 LHe ASSEMBLY

significantly to the total helium boil-off of a large magnet. CCM has 70 m^2 of surface area for heat exchange. Special efforts were taken to provide high quality thermal insulation. Following a technique developed by the author,⁴ twelve layers of 500 \AA NRC-2 multilayer insulation were wrapped around the helium shells whose surfaces were previously covered with a reflective aluminum tape (3M #425). This method was measured to give a heat transfer rate of 15 mW/m^2 , which is better than the 40 mW/m^2 usually used for magnet design. Between the radiation shield (78K) and the vacuum shell (300K), 40 layers of 300 \AA NRC-2 were used.

Power Chimney and Instrumentation

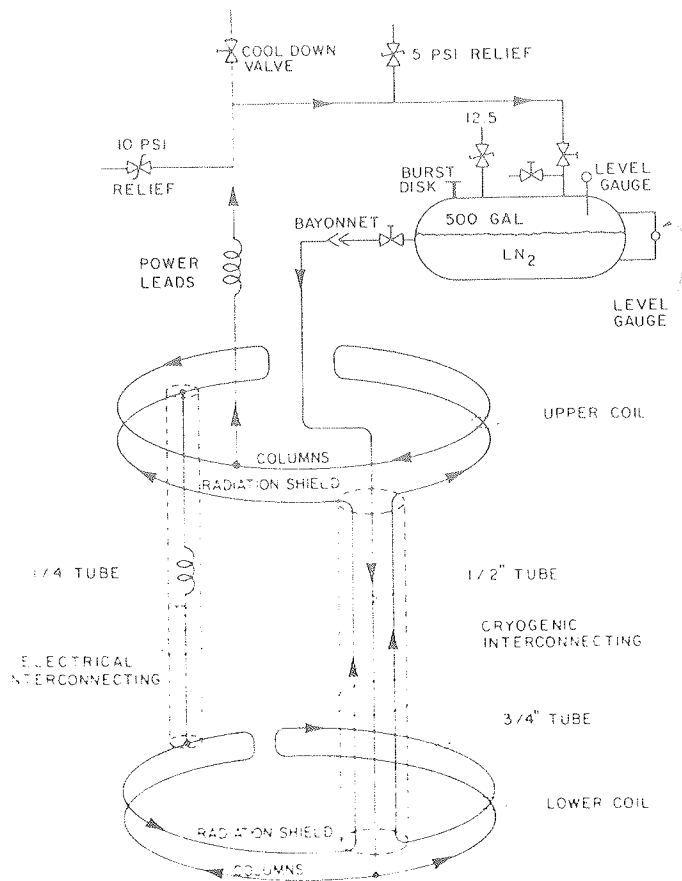
The two coils are connected electrically and cryogenically together through two 7.62 cm interconnecting tubes, and the single chimney reduces conduction heat transfer from the outside world. Maximum operating current is 1000 A for CCM and the coils are powered through a pair of AMI leads^{5,6} rated for 1625 A operation.

A fairly comprehensive protective system has been developed. CCM would automatically discharge and dump its energy into an external dump resistor (0.2 Ω) whenever one of the following conditions is detected:

- 1) Magnet ground current (possible short to ground)
- 2) Over current on magnet
- 3) Excessive voltage on current leads
- 4) Low LHe boil-off rate
- 5) High LHe boil-off rate
- 6) LHe level I (low LHe level or failure of probe)
- 7) LHe level II (low LHe level or failure of probe)
- 8) Overheating of the diode in the power supply
- 9) Improper access into the experimental radiation area

Cryogenic Test Results

Following a construction period of 2 years, the magnet (Fig. 7) was ready for pump down, a cool down and a low current test before installation into the CCM iron. The high humidity at the construction site (Meson Area Detector Building) during superinsulation and cold-shock leak checking of the shells made the pump down a long and tedious process. In the end, we removed the

Fig. 5 LN₂ SYSTEM

15.24 cm (6") burst disk on the upper vacuum shell and pumped with a 10.16 cm (4") cold trap and diffusion pump. Approximately 12 liters of water were removed from the system. Several small leaks in the vacuum shell were detected and readily fixed. (The vacuum shell contained over 1000 linear feet of weldment.)

We started cooldown when the vacuum read ~ 100 millitorrs. Figure 8 shows the rate at which the two coils were cooled down. A liquid nitrogen precooling technique was used, which permitted both coils to be immersed in LN₂ before further cooling down with LHe. The total cryogen requirement was ~ 4000 l of LN₂ and ~ 3000 l of LHe. If we had cooled the coils down to only 90K instead of 78K, an additional 5500 l of LHe would have been required for the cooldown.

The LHe boil-off rate was monitored for ~ 5 days. It is estimated (Fig. 9) that the boil-off rate will eventually settle down at ~ 13 l/hr. Since the intercepts on the columns were running at 105K instead of the anticipated 80K, the LHe usage rate should be ~ 10 -11 l/hr, after a higher pressure head is applied to the LN₂ cooling system. This is in reasonable agreement with the ~ 8 l/hr as predicted by calculation. Also, since this value is substantially less than the break-even value of 40 l/hr, the cryogenic performance is considered successful.

We then passed 10A through the coils. No ground shorts were detected. Various interlocks were also checked out. Unfortunately, we cannot fully charge the magnet to 1000 A until we have the coils installed in the CCM magnet iron. We had to warm up sooner than we would have liked to (before we can take all LHe boil-off data) because of a scheduling problem.

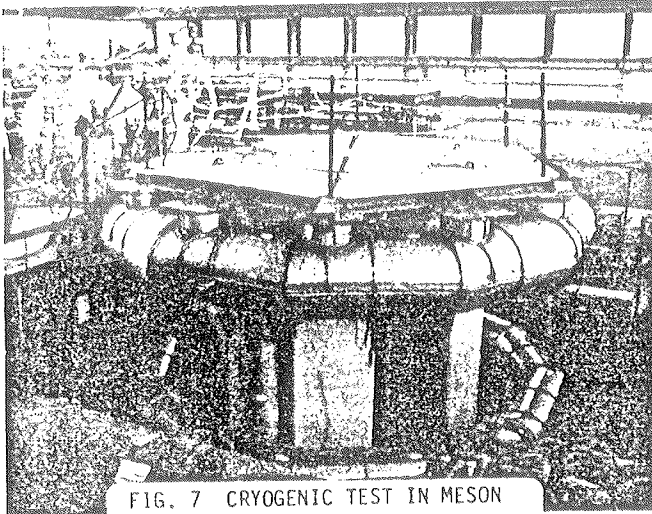
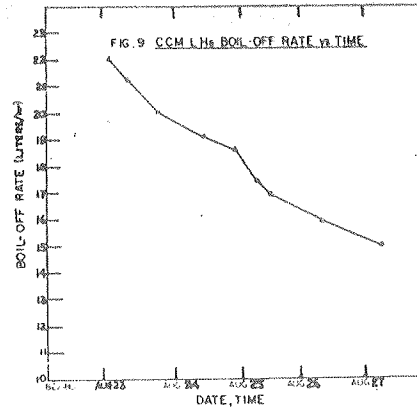
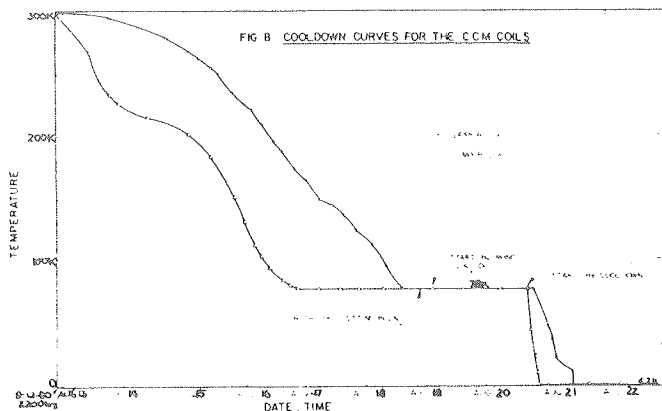


FIG. 7 CRYOGENIC TEST IN MESON



Future Plan

The Meson Test indicated that the superconducting coils are economically viable for the replacement of the old copper coils. The old coils are being removed from the Muon Lab. The CCM superconducting coils are expected to be fully charged in Dec. 1980 or Jan. 1981.

Acknowledgments

Special thanks should go to Howard Hart, Eugene Smith, John Rauch, Ed Tilles, Jim Michelassi, Albert Ito, Jim Peifer, Mike McKenna and in particular, Charles P. Grozis, for their dedications in various stages of the construction and design of the superconducting CCM. We are also indebted to all the personnel involved in the project, from the Research Services Department, Technical Services Section and the Village Machine and Weld Shop at Fermilab.

References

1. Robert Lari, "Graphic, Time-sharing Magnet Design Computer Programs at ANL," Proc. 5th Int. Conf. on Magnet Technology, Rome (1975) p. 244-251.
2. C.W. Trowbridge, Proc. 4th Int. Conf. on Magnet Technology, Brookhaven (1972), p. 555.
3. E.M.W. Leung, "Magnetic Field Calculation of the Superconducting Version of the Chicago Cyclotron Magnet using GFUN-3D", FNAL TM-759 2751.000 (1978).
4. E.M.W. Leung, R.W. Fast, H.L. Hart and J.R. Heim, "Techniques for Reducing Radiation Heat Transfer Between 77 & 4.2K", Advances in Cryogenic Engineering, Vol. 25, p. 429 (1980).
5. Manufactured by the American Magnetics Inc.
6. K.R. Efferson, The Review of Scientific Instruments, Vol. 38, No. 12, p. 1776-1779, Dec. 1967.

Appendix A4

TITLE: Determining the Maximum Expected Pressure in the Vacuum Jacket Should the Helium Reservoir Rupture

AUTHOR: R.I. Dachniwskyj, M. Stone

DATE: July 29, 1985

OBJECTIVE: To determine the maximum pressure that the vacuum jacket would experience if the helium reservoir should rupture.

REFERENCE: CCI Report #571-1000, - Relief valve sizing for CDF solenoid quench, available upon request.

ASSUMPTIONS

1. The helium reservoir completely splits open at 30 psid, dumping its contents into the evacuated vacuum space.
2. The change in enthalpy of the vacuum shell and vent pipes is neglected during venting.
3. The heat transfer is taken to occur across the entire area of the vacuum shell.
4. None of the heat flux (energy) goes into warming up the nitrogen shield, superinsulation or the helium cryostat.
5. The energy transfer to the helium as the nitrogen shield is cooled is ignored.
6. Ignore volume taken up by the columns.
7. Starting conditions.

$$M_{\text{He}} = 2.5 \times 10^5 \text{ g}$$

$$P_i = 1.8 \text{ atm abs}$$

$$x = 0.0, \text{ or } 100\% \text{ liquid}$$

These starting conditions were chosen because they give the maximum initial venting rate if the helium reservoir should rupture.

8. The vents are uninsulated.
9. The vacuum jacket is a toroid.
10. All calculations assume steady state.

PARAMETERS

Determining volume of the vacuum jacket, interior volume of vacuum jacket

$$V_I = \frac{\pi D_{UC}^2}{4} \times \pi D_{MU} + \frac{\pi D_{LC}^2}{4} \times \pi D_{ML}$$

$$D_{UC} = 36 \text{ in} \quad \text{minor diameter of upper coil}$$

$$D_{MU} = 206 \text{ in} \quad \text{major diameter of upper coil}$$

$$D_{LC} = 24 \text{ in} \quad \text{minor diameter of lower coil}$$

$$D_{ML} = 192 \text{ in} \quad \text{major diameter of lower coil}$$

$$V_I = 9.32 \times 10^5 \text{ in}^3$$

$$= 1.53 \times 10^7 \text{ cm}^3$$

VOLUME OF HELIUM CRYOSTAT

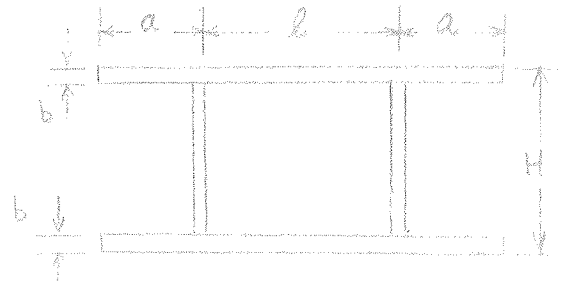
$$V_C = \pi (D_{MU} + D_{ML})[(l \cdot H) + (4)(a)(b)]$$

$$= (\pi)(206 + 192)[(9.625)(7.55) + (4)(0.3125)(1.44)]$$

$$= 9.32 \times 10^4 \text{ in}^3$$

$$= 1.5 \times 10^6 \text{ cm}^3$$

Dimensions are from Appendix A2
of the Safety Manual, pg. 148



VOLUME OF METAL IN HELIUM RESERVOIR

$$V_R = (\pi)(D_{MU})(t)(l)$$

$$= \pi(206)(0.3125)(63.2)$$

$$= 1.28 \times 10^4 \text{ in}^3$$

$$= 2.10 \times 10^5 \text{ cm}^3$$

t = thickness of stainless steel
plate that the reservoir is
construction of

l = perimeter of the reservoir

VOLUME OF SUPERINSULATION (crude estimation)

N = number of layers - 60 on the nitrogen shield

$$V_S = (\pi)(D_{UC})(t_M)(\pi)(D_{MU})(N) + \pi(D_{LC})(t_M)(\pi)(D_{LU})(N)$$

$$= (\pi)(36)(0.00025)(\pi)(206)(60) + \pi(24)(0.00025)(\pi)(192)(60)$$

$$= 1.78 \times 10^3 \text{ in}^3$$

$$= 2.92 \times 10^4 \text{ cm}^3$$

Actual unoccupied volume of the vacuum jacket

$$\begin{array}{r}
 1.51 \times 10^7 \\
 -1.53 \times 10^6 \\
 -2.10 \times 10^5 \\
 -2.92 \times 10^4 \\
 \hline
 1.33 \times 10^7 \text{ cm}^3
 \end{array}$$

AREA OF VACUUM JACKET

$$\begin{aligned}
 A &= (\pi)(D_{UC})(\pi)(D_{MU}) + (\pi)(D_{LC})(\pi)(D_{LU}) \\
 A &= \pi^2(36)(206) + \pi^2(24)(192) \\
 &= 1.19 \times 10^5 \text{ in}^2 \\
 &= 826 \text{ ft}^2
 \end{aligned}$$

DETERMINING HEAT LOAD TO THE HELIUM GAS

The CCM vacuum jacket for this heat transfer analysis is being modeled as a large horizontal nitrogen condensing pipe having cold helium gas flowing through it. To determine the quantity of heat transferred to the cold helium gas the following three thermal resistances must be calculated:

1. The nitrogen condensation convective thermal resistance (i.e. the condensation load).
2. The conductive thermal resistance of the stainless steel vacuum jacket.
3. The thermal resistance (convective in nature) present in getting the energy from the stainless steel vacuum jacket into the flowing helium gas.

The nitrogen condensation convective thermal resistance

$$= 1/hA$$

$$h = \text{convection heat transfer coefficient for condensation on horizontal pipes from the handbook of Heat Transfer by Rohsenow and Hartnet, pg 12-16.} = 0.728 \frac{g\rho(\rho-\rho_v)K^3 h_{fg}}{D\mu\Delta T}^{1/4}$$

$$\text{BTU/HR-FT}^2\text{-R}$$

$$A = \text{area of the vacuum jacket} = 826 \text{ FT}^2$$

$$g = \text{acceleration of gravity} = 4.17 \times 10^8 \text{ FT/HR}^2$$

$$\rho = \text{density of liquid nitrogen} = 50.5 \text{ LB/FT}^3 \text{ at 1 atm-abs}$$

$$\rho_v = \text{density of saturated nitrogen vapor} = 0.288 \text{ LB/FT}^3$$

$$K = \text{thermal conductivity of the liquid} = 0.0787 \text{ BTU/HR-FT-R}$$

$$h_{fg} = h_{fg} + 3/8 C (T_S - T_W)$$

$$h_{fg} = \text{latent heat} = 85.4 \text{ BTU/LB}$$

$$C = \text{specific heat of liquid nitrogen at condensed pressure} = 0.493 \text{ BTU/LB-R}$$

$$T_S = \text{saturation temperature} = 139.2 \text{ R}$$

$$T_W = \text{cold surface temperature} = 11 \text{ R}$$

$$D = \text{diameter of tube} = 2 \text{ FT}$$

$$\mu = \text{viscosity of liquid nitrogen 1 atm-abs} = 0.396 \text{ LB/FT-HR}$$

$$\Delta T = T_S - T_W = 128.2 \text{ R}$$

$$\therefore h = 0.728 \frac{(4.17 \times 10^8)(50.5)(50.5 - 0.288)(0.0787)^3(109)}{(2)(0.396)(128.2)}^{1/4}$$

$$h = 112 \frac{\text{BTU}}{\text{HR-FT}^2\text{-R}}$$

Therefore the nitrogen condensation convective thermal resistance [NC] = $1/(112)(826) = 1.08 \times 10^{-5}$ HR-R/BTU.

The conductive thermal resistance [CTR] of the stainless steel vacuum jacket

$$= \frac{k_n (r_o/r_i)}{2\pi K_{\text{avg}} L},$$

from Engineering Heat Transfer by Karlekar and Desmond.

r_o = outside radius of the vacuum jacket = 18 in

r_i = inside radius of the vacuum jacket = 17.875 in

K_{avg} = thermal conductivity of the stainless steel at $[11 + 138.2]/2 = 75 \text{ R} = 2.66 \text{ BTU/HR-FT-R}$

From LNG Materials and Fluids Data

L = length of cylinder = $\frac{\pi(D_{\text{MU}})}{12} = \frac{(\pi)(206)}{12} = 54 \text{ ft}$

$$\begin{aligned} \therefore \text{CTR} &= \frac{k_n (18/17.875)}{(2)(\pi)(2.66)(54)} \\ &= 7.72 \times 10^{-6} \text{ HR-R/BTU} \end{aligned}$$

The convective thermal resistance of the flowing helium [CTR_H] gas with the vacuum jacket equals $1/h_{\text{CTR}_H} A$. To determine h_{CTR_H} , the Nusselt number $NU = 0.022 (R_e)^{0.8} (P_r)^{0.4}$ for fully established turbulent flow in a circular tube, fully developed constant heat rate, (from "The Handbook of Heat Transfer" by Rohsenow and Hartnett, pg. 7-33), must be calculated. To determine the Nusselt number the Reynolds and Prandtl number for the flowing helium must be determined, as given below. It must be shown later that the following initial guess of the helium gas properties were good.

$P_r = 0.936$ He at $P = 1.8 \text{ atm-abs}$

$T = 6.0 \text{ }^\circ\text{K}$

$$R_e = \frac{(6.31)(W)}{d\mu}$$

$W = \text{flow rate} = 7.94 \times 10^4 \text{ [LB/HR]}$

Initial
Guess

$d = 36 \text{ [IN]}$

$\mu = 17.0 \times 10^{-4} \text{ centipoise}$

$$\therefore R_e = 8.2 \times 10^6$$

$$\therefore N_u = (0.022)(8.2 \times 10^6)^{0.8} (0.936)^{0.6} = 7.182 \times 10^3$$

K = thermal conductive of the helium gas = 7.69×10^{-3} BTU/HR-FT-R

D = diameter of circular pipe = 3.0 FT

$$N_u = \frac{(h_{CTR}) (D)}{K} = 7.10$$

$$\therefore h_{CTR} = 18.4 \text{ BTU/HR-FT}^2\text{-R}$$

$$CTR_H = \frac{1}{h_{CTR} A} = \frac{1}{(18.4)(826)} = 6.58 \times 10^{-5} \frac{\text{HR-R}}{\text{BTU}}$$

The heat load to the helium gas equals

$$\begin{aligned} Q &= \frac{\Delta T}{NC + CTR + CRTH} \\ &= \frac{128.2}{1.08 \times 10^{-5} + 7.72 \times 10^{-6} + 6.58 \times 10^{-5}} \\ &= 1.54 \times 10^6 \text{ BTU/HR} \\ &= 4.50 \times 10^5 \text{ [W]} \end{aligned}$$

Determining mass flow from the vacuum vessel after the helium reservoir has ruptured.

$$\begin{aligned} \text{specific volume of helium} &= \frac{1.33 \times 10^7 \text{ cm}^3}{2.5 \times 10^5 \text{ g}} \\ \text{after the reservoir} & \\ \text{ruptures} & \\ &= 53.2 \text{ cm}^3/\text{g} \end{aligned}$$

At 1.8 atm-abs the temperature of the helium with the above specific volume is 5.98 K. The mass flow with time is given in Table I. The method used in Table I to determine the mass flow rate is explained in CCI Report No. 571-1000.

DETERMINING PRESSURE DROP IN VACUUM AND HELIUM VENT LINES

Components list for:

8-inch Fike rupture disk to the outside upper coil vacuum jacket.

TABLE I. Flow Rate of He Through Relief Valve Versus Time

	0.0	0.2	0.4	0.6	0.8	1.0	1.5	2.0	2.5	3.0	5	10	15	30
Time elapsed from initiation of flow through vacuum vent (sec)	1.8	1.8	1.8	1.8	1.8	1.8	1.8	1.8	1.8	1.8	1.8	1.8	1.8	1.8
Vacuum jacket pressure (ATMA)	0	9.0×10^4	2.26×10^5	2.26×10^5	2.26×10^5	2.26×10^5	9.05×10^5	2.26×10^6	2.26×10^6	6.78×10^6				
Energy absorbed by He (J) ($\rho = 4.4 \times 10^5$ W)	39.12	39.48	39.90	40.27	40.65	41.03	42.03	43.03	44.13	45.23	49.83	63.23	81.43	156.7
Enthalpy of helium (J/g)	5.98	6.03	6.09	6.15	6.20	6.26	6.4	7.05	7.22	7.38	7.63	9.94	13.26	27.45
Temperature of helium ($^{\circ}$ K)	53.2	54.0	54.9	55.78	56.64	57.49	59.75	62.0	64.47	66.69	77.3	107.24	147.7	313.5
Specific volume of helium (cm^3/g)	2.5×10^5	2.46×10^5	2.42×10^5	2.38×10^5	2.34×10^5	2.31×10^5	2.23×10^5	2.15×10^5	2.06×10^5	1.99×10^5	1.72×10^5	1.26×10^5	9.0×10^4	4.24×10^4
Mass of helium in the vacuum jacket (G)	0	2.0×10^6	2.0×10^6	2.0×10^6	2.0×10^6	1.5×10^6	1.6×10^6	1.6×10^6	1.8×10^6	1.4×10^6	1.4×10^6	9.60×10^3	6.8×10^3	3.17×10^3
Mass leaving the coil (g/s)	0	44.1	44.1	44.1	44.1	33.1	35.73	35.3	39.7	30.39	30.9	21.1	14.9	6.9
Mass leaving the coil lb/s	0	0.36	0.37	0.37	0.38	0.38	1.0	1.0	1.1	1.1	4.6	13.4	18.2	75.3
Δ Enthalpy of helium														

<u>Item</u>	<u>L/D</u>	<u>Equivalent Length</u>
Entrance - 8-inch	(58)	40
8-inch straight pipe		18
8-inch bellows (2)-1.5 bellows		12
8-inch check valve		37
8-inch elbow 90 ^o	(31)	22
8-inch check valve		35
8-inch x 12 inch expander	(17)	12
TOTAL		176 FT
12-inch - tee flow thru run	(23)	24
12-inch straight pipe		30
12-inch - 90 ^o elbow (3)	(31)	96
12-inch bellows (1)-1.5		6
12-inch pipe exit	(78)	81
TOTAL		237 FT

Component list for:

4-inch Fike rupture disk to the outside-lower coil vacuum jacket.

<u>Item</u>	<u>L/D</u>	<u>Equivalent Length</u>
4-inch entrance	(48)	17
4-inch straight pipe		2
4-inch 90° elbow (3)	(31)	33
4-inch by 8-inch expander	(20)	7
TOTAL		59
8-inch straight pipe		23
8-inch bellows (1)-1.5		6
8-inch check valve		37
8-inch by 12-inch expander	(17)	12
8-inch check valve		35
8-inch 90° elbow	(31)	22
TOTAL		135
12-inch straight pipe		30
12-inch tee flow thru branch	(60)	62
12-inch 90° elbows (3)	(31)	96
12-inch bellows (1)-1.5		6
12-inch pipe exit	(78)	81
TOTAL		275

Component list for:

East helium leg - 4-inch Fike rupture disk to the outside helium reservoir.

(4" vent piping)

<u>Item</u>	<u>L/D</u>	<u>Equivalent Length</u>
5-inch entrance to chimney	50	21
5-inch straight tube up the chimney		~3 full flow
entrance into top hat	65	27
TOTAL		51 FT
exit from top hat into 4" Sch 10 pipe	48	17
4-inch elbow	31	11 half flow
straight section of 4-inch pipe		~3
4-inch x 78-inch expander	20	7
TOTAL		38 FT
(8" vent piping)		
8-inch by 12-inch expander	17	12
TOTAL		12 FT
(12" vent piping)		
12-inch bellows (2) 1.5 ft		12
straight run of 12-inch Sch 10 pipe		56
90° 12-inch Sch 10 elbows (2)	31	64
12-inch exit into vent chimney	80	83
12-inch tee branch flow	60	62
TOTAL		277 FT

Components list for:

West helium leg - 4-inch Fike rupture disk to the outside helium reservoir.
Piping is the same except for as follows:

(12-inch vent piping)

<u>Item</u>	<u>L/D</u>	<u>Equivalent Length</u>
90° square elbow	60	62
12-inch tee flow thru run instead of through branch	20	21
Total from above 12-inch piping minus tee		215
TOTAL		298 FT

The pressure drop for compressible flow per 100 feet of vent piping =

$$\Delta P_{100} = \frac{3.36 \times 10^{-4} \cdot f \cdot W^2}{\rho_{\text{avg}} d^5}$$

W = LB/HR

ρ_{avg} = density LB/FT³

d = diameter of pipe in

f = friction factor

The helium flowing through the vent lines can be warmed by two sources, condensation and the energy contained within the stainless steel vent line. The energy absorbed by a bare line exposed to the ambient $Q=7.3 \times 10^3$ [W]. Reference NBS monogram. The energy contained within the stainless steel pipe equals 76.6 [J/g].

Surface area (SA) of vacuum vent line

$$SA_8 = \pi DL = \frac{\pi(8.625)(56)}{12} = 126 \text{ FT}^2$$

$$SA_{12} = \pi DL = \frac{\pi(12.75)(42)}{12} = 140 \text{ FT}^2$$

Heat absorbed by the helium in the vacuum vent line due to condensation.

$$\begin{aligned} \dot{q} &= (7.3 \times 10^3)(140 + 126) \\ &= 1.94 \times 10^6 \text{ W} \end{aligned}$$

The energy absorbed by the helium from the vacuum vent pipe.

$$N_{\mu} = 0.022 (R_e)^{0.8} (P_r)^{0.4}$$

$$R_e = \frac{(6.31)(W)}{d\mu}$$

$W = 1.13 \times 10^5 \text{ LB/HR}$
 8-12-V
 +
 4-12-V

$$W = 9.1 \times 10^4 \text{ LB/HR}$$

8-8-V

$$W = 2.2 \times 10^4 \text{ LB/HR}$$

4-8-V

$$\mu = 46.6 \times 10^{-4} \text{ centipoise}$$

Viscosity at $p = 1.8 \text{ atm-abs}$
 $P_r = 0.711 \quad T_{AVG} = 30^{\circ}\text{K}$

$$\therefore R_e = \frac{(1.13 \times 10^5)(6.31)}{(12.4)(46.6 \times 10^{-4})} = 1.23 \times 10^7$$

+
4-12-V

$$\therefore R_e = \frac{(9.1 \times 10^4)(6.31)}{(8.3)(46.6 \times 10^{-4})} = 1.48 \times 10^7$$

$$\therefore R_e = \frac{(2.2 \times 10^4)(6.31)}{(4.26)(46.6 \times 10^{-4})} = 6.99 \times 10^6$$

$$N_{u_{8-12-V}} = (0.022)(1.23 \times 10^7)^{0.8} (0.711)^{0.4} = 9.02 \times 10^3$$

4-12-V

$$N_{u_{8-8-V}} = (0.022)(1.48 \times 10^7)^{0.8} (0.711)^{0.4} = 1.05 \times 10^4$$

$$N_{u_{4-8-V}} = (0.022)(6.99 \times 10^6)^{0.8} (0.711)^{0.4} = 5.74 \times 10^3$$

$$N_u = \frac{hd}{K} \quad K_{AVG} = \text{Average thermal conductivity of the flowing gas}$$

$$\therefore h = \frac{N_u K_{AVG}}{d} \quad \therefore K_{AVG} = 1.98 \times 10^{-2} \frac{\text{BTU}}{\text{HR-FT-R}}$$

$$h_{\substack{8-12-V \\ 4-12-V}} = \frac{(9.02 \times 10^3)(1.98 \times 10^{-2})}{1.03} = 173 \frac{\text{BTU}}{\text{HR-FT}^2\text{-R}}$$

$$h_{8-8-V} = \frac{(1.05 \times 10^4)(1.98 \times 10^{-2})}{0.692} = 300 \frac{\text{BTU}}{\text{HR-FT}^2\text{-R}}$$

$$h_{4-8-V} = \frac{(5.74 \times 10^3)(1.98 \times 10^{-2})}{0.355} = 320 \frac{\text{BTU}}{\text{HR-FT}^2\text{-R}}$$

ΔT = The log mean avg between the ambient and inside temperature of the helium gas = 200°K

$$Q = hA\Delta T$$

A = Area of vent line

$$\Delta T = 300^{\circ}\text{K}$$

$$Q_{\substack{8-12-V \\ 4-12-V}} = (173)(200)(140) = 4.84 \times 10^6 \text{ BTU/HR}$$

$$Q_{8-8-V} = (300)(200)(79) = 4.74 \times 10^6 \text{ BTU/HR}$$

$$Q_{4-8-V} = (200)(96)(320) \\ = 6.14 \times 10^6 \text{ BTU/HR}$$

$$Q_T = 1.57 \times 10^7 \text{ BTU/HR} \quad \text{Total amount of heat absorbed from the vent pipe by the flowing helium.} \\ = 4.59 \times 10^6 \text{ W}$$

Surface area of helium vent lines

$$SA_{12} = \pi DL = \frac{\pi(12.75)(56)}{12} = 187 \text{ FT}^2$$

$$SA_4 = \pi DL = \frac{\pi(4.625)(8)}{12} = 10 \text{ FT}^2$$

Heat absorbed by the helium in the helium vent line due to condensation

$$= \dot{q} = (7.3 \times 10^3)(187 + 10) \\ = 1.44 \times 10^6 \text{ W}$$

The energy absorbed from the helium vent line by the helium.

$$N_u = 0.022 (R_c)^{0.8} (P_r)^{0.4}$$

$$R_e = \frac{(6.31)(W)}{d\mu}$$

$$W_{4-4-H_e} = 2.2 \times 10^4 \text{ LB/HR}$$

$$W_{4-12-H_e} = 4.4 \times 10^4 \text{ LB/HR}$$

$$P = 1.8 \text{ Atm-abs}$$

$$T_{AVG} = 25^\circ\text{K}$$

$$P_r = 0.710$$

$$u_{AVG} = 41.6 \times 10^{-4} \text{ centipoise}$$

$$\therefore R_{4-4-H_e} = \frac{(2.2 \times 10^4)(6.31)}{(4.260)(41.6 \times 10^{-4})} = 7.83 \times 10^6$$

$$\therefore R_{e4-12-H} = \frac{(4.4 \times 10^4)(6.31)}{c(12.4)(41.6 \times 10^{-4})} = 5.38 \times 10^6$$

$$\therefore N_{u4-4-H_e} = (0.022)(7.83 \times 10^6)^{0.8} (0.711)^{0.4} \\ = 6.28 \times 10^3$$

$$N_{u_{4-12-H_e}} = (0.022)(5.38 \times 10^6)^{0.8}(0.711)^{0.4}$$

$$= 4.65 \times 10^3$$

$$N_u = \frac{hd}{K_{avg}} \quad K_{AVG} = \text{average thermal conductivity of the flowing He gas}$$

$$K_{AVG} = 1.78 \times 10^{-2} \frac{\text{BTU}}{\text{HR-FT-R}}$$

$$h_{4-4-H_e} = \frac{(6.28 \times 10^3)(1.78 \times 10^{-2})}{0.355} = 315 \frac{\text{BTU}}{\text{HR-FT}^2\text{-R}}$$

$$h_{4-12-H_e} = \frac{(4.65 \times 10^3)(1.78 \times 10^{-2})}{1.03} = 80 \frac{\text{BTU}}{\text{HR-FT}^2\text{-R}}$$

$$Q = hA\Delta T$$

ΔT = the log mean average between the ambient and the inside temperature of the helium gas = 200°K

$$Q_{4-4-H_e} = (315)(200)(0) = 6.30 \times 10^5 \text{ BTU/HR}$$

$$Q_{4-12-H_e} = (80)(200)(187) = 2.99 \times 10^6 \text{ BTU/HR}$$

$$Q_T = 3.62 \times 10^6 \text{ BTU/HR}$$

$$= 1.66 \times 10^6 \text{ W}$$

MASS FLOW THROUGH EACH RUPTURE DISK

The flow through each rupture disk is proportional to each disk's area if the pressure drop in each vent line is the same.

$$W_A = \text{mass flow} \quad W_8 = 9.55 \times 10^4 \text{ LB/HR} = 1.57 \times 10^4 \text{ g/s}$$

$$A = \text{which rupture disk} \quad W_4 = 2.31 \times 10^4 \text{ LB/HR} = 2.91 \times 10^3 \text{ g/s}$$

Change in enthalpy: For the vacuum vent line helium due to cooling the vent line. Condensation load cannot occur until the vent line is cooled down to 77° , therefore, the heat rate is reduced to the condensation load.

$$\Delta H = \frac{4.59 \times 10^6 \text{ J/s}}{1.5 \times 10^4 + 2.77 \times 10^3 \text{ g/s}}$$

$$= 258 \text{ J/g}$$

Change in enthalpy: For the helium vent line helium gas due to cooling of the vent line. Condensation load cannot occur until the vent line is cooled down to 77°K , by this time over 90% of the stored energy in the vent line has been removed. Therefore, the heat rate is reduced to the condensation load.

$$= \frac{1.06 \times 10^6 \text{ J/s}}{(2)(2.77 \times 10^3) \text{ g/s}}$$

$$= 191 \text{ J/g}$$

Finding the helium gas exit temperature

$$\text{Initial enthalpy of the gas} = 39.2 \text{ J/g}$$

Final enthalpy at vacuum vent exit

$$= 39.2 + 258 = 298 \text{ J/g}$$

$$\therefore \text{exit temperature} = 55^{\circ}\text{K}$$

$$\therefore T_{\text{AVG}} = \frac{6 + 515}{2} = 30 \quad \text{close to intide guess of } 30^{\circ}\text{K}$$

$$\therefore (\text{avg} = 0.182 \text{ LF/FT}^3)$$

$$\therefore \mu_{\text{avg}} = 46.6 \times 10^{-4} \text{ centipoise}$$

Final enthalpy at helium vent exit

$$= 39.2 + 191 = 230 \text{ J/g}$$

$$\therefore \text{exit temperature} = 41^{\circ}\text{K}$$

$$\therefore T_{\text{AVG}} = \frac{6 + 41}{2} = 23.5^{\circ}\text{K} \quad \text{close to initial guess of } 25^{\circ}\text{K}$$

$$\therefore \rho_{\text{avg}} = 0.233 \text{ lb/ft}^2$$

$$\therefore \mu_{\text{avg}} = 40 \times 10^{-4} \text{ centipoise}$$

Determining the friction factor

$$R_e = \frac{(6.31)(W)}{d\mu}$$

μ = viscosity centipoise
 d = diameter in
 W = mass flow lb/hr

$$R_{e \text{ 8-8-V}} = \frac{(6.31)(9.1 \times 10^4)}{(8.3)(46.6 \times 10^{-4})} = 1.48 \times 10^7 \quad \therefore f_{\text{8-8-V}} = 0.014$$

$$R_{e \text{ 8-12-V}} = \frac{(6.31)(1.13 \times 10^5)}{(12.4)(46.6 \times 10^{-4})} = 1.23 \times 10^7 \quad \therefore f_{\text{8-12-V}} = 0.013$$

$$R_{e \text{ 4-12-V}}$$

$$R_{e \text{ 4-4-V}} = \frac{(6.31)(2.2 \times 10^4)}{(4.260)(46.6 \times 10^{-4})} = 0.70 \times 10^7 \quad \therefore f_{\text{4-4-V}} = 0.016$$

$$R_{e \text{ 4-8-V}} = \frac{(6.31)(2.2 \times 10^4)}{(8.3)(46.6 \times 10^{-4})} = 3.59 \times 10^6 \quad \therefore f_{\text{4-8-V}} = 0.014$$

$$R_{e \text{ 4-5-He}} = \frac{(6.31)(4.4 \times 10^4)}{(5.0)(40 \times 10^{-4})} = 1.39 \times 10^7 \quad \therefore f_{\text{4-5-He}} = 0.0155$$

$$R_{e \text{ 4-4-He}} = \frac{(6.31)(2.2 \times 10^4)}{(4.260)(40 \times 10^{-4})} = 8.16 \times 10^6 \quad \therefore f_{\text{4-4-He}} = 0.016$$

$$R_{e \text{ 4-8-He}} = \frac{(6.31)(2.2 \times 10^4)}{(8.33)(40 \times 10^{-4})} = 4.17 \times 10^6 \quad \therefore f_{\text{4-8-He}} = 0.014$$

$$R_{e \text{ 4-12-He}} = \frac{(6.31)(4.4 \times 10^4)}{(12.4)(40 \times 10^{-4})} = 5.62 \times 10^6 \quad \therefore f_{\text{4-12-He}} = 0.013$$

Pressure drop in the vent piping

$$\Delta P_{\text{100 8-8-V}} = \frac{(3.36 \times 10^{-4})(0.014)(9.1 \times 10^4)^2}{(0.182)(8.3)5} = 5.42 \text{ PSI/100 FT}$$

$$\Delta P_{\text{100 8-12-V}} = \frac{(3.36 \times 10^{-4})(0.013)(1.13 \times 10^5)^2}{(0.182)(12.4)5} = 1.06 \text{ PSI/100 FT}$$

$$\Delta P_{\text{100 4-12-V}}$$

$$\Delta P_{100}^{4-4-V} = \frac{(3.36 \times 10^{-4})(0.016)(2.2 \times 10^4)^2}{(0.182)(4.26)^5} = 10.16 \text{ PSI/100 FT}$$

$$\Delta P_{100}^{4-8-V} = \frac{(3.36 \times 10^{-4})(0.014)(2.2 \times 10^4)^2}{(0.182)(8.3)^5} = 0.32 \text{ PSI/100 FT}$$

$$\Delta P_{100}^{4-3-He} = \frac{(3.36 \times 10^{-4})(0.0155)(4.4 \times 10^4)^2}{(0.233)(5.0)^5} = 12.11 \text{ PSI/100 FT}$$

$$\Delta P_{100}^{4-4-He} = \frac{(3.36 \times 10^{-4})(0.016)(2.2 \times 10^4)^2}{(0.233)(4.260)^5} = 6.95 \text{ PSI/100 FT}$$

$$\Delta P_{100}^{4-8-He} = \frac{(3.36 \times 10^{-4})(0.014)(2.2 \times 10^4)^2}{(0.233)(8.3)^5} = 0.217 \text{ PSI/100 FT}$$

$$\Delta P_{100}^{4-12-He} = \frac{(3.36 \times 10^{-4})(0.013)(4.4 \times 10^4)^2}{(0.233)(12.4)^5} = 0.107 \text{ PSI/100 FT}$$

Pressure drop for the 8-inch vacuum space rupture disk to the outside

$$= (1.76)(5.42) + (1.06)(2.37) = 12.0 \text{ PSI}$$

Pressure drop for the 4-inch vacuum space rupture disk to the outside

$$= (0.59)(10.16) + (1.35)(0.32) + (2.75)(1.06)$$

$$= 9.34 \text{ PSI}$$

Pressure drop for the 4-inch east side helium rupture disk to the outside

$$= (0.51)(12.11) + (0.38)(6.95) + (0.12)(0.217) + (2.8)(0.107)$$

$$= 9.14 \text{ PSI}$$

Pressure drop for the 4-inch west side helium rupture disk to the outside

$$= (0.51)(12.11) + (0.38)(6.95) + (0.12)(0.217) + (3)(0.107)$$

$$= 9.16 \text{ PSI}$$

PRESSURE DROP ACROSS FIKE RUPTURE DISK

The vacuum vessel is protected from an overpressure by a 8-inch and three 4-inch Fike rupture disks, the pressure settings are as follows: 8-inch - 11.1 psid, 4-inch lower coil vacuum space - 12.3 psid, and the two 4-inch helium

rupture disks - 11.7 psid. To calculate the flow through a Fike rupture disk the following equation is used.

$$A = \frac{W}{K C_1 P_O} \sqrt{\frac{t + 460}{M}}$$

$$A = \text{flow area} = \pi(8)^2/4 + (3)\pi(4)^2/4 = 88 \text{ in}^2$$

$$W = \text{flow rate lb/s} = 44.1 \text{ lb/s}$$

$$K = 0.62 \text{ ASME coefficient}$$

$$C_1 = 0.0744$$

$$t = \text{temperature of flow media } ^\circ\text{F} = -451^\circ\text{F}$$

$$M = \text{molecular weight} = 4$$

$$P_O = \text{pressure} = ?$$

$$\therefore P_O = 18 \text{ psia}$$

CONCLUSIONS

1. Maximum pressure in the vacuum jacket should the helium reservoir rupture = $12.0 + 3.3 = \underline{15.3 \text{ PSID}}$.
2. The assumption that the pressure in the vacuum jacket was 1.8 atm-abs is valid because the actual pressure is 2.04 atm-abs.
3. Proportioning the flows by the area of the individual rupture disk is valid because the pressure drop in vents is approximately the same.

Appendix - A5

TITLE: Description of the vacuum jacket test, test procedure and test results

DATE: July 25, 1985

AUTHOR: Roman I. Dachniwskyj

OBJECT: To verify that the stress intensity seen by the vacuum jacket during the pressure test does not exceed the code allowable stress intensity for 304 stainless steel by 50%.

EQUIPMENT:

1. SR4 BLH 60⁰ Delta rosette model #FAER-25D-35-S13EL and model #FAER-25D-35-S6EL.
2. Vishay V/E-20 strain gage indicator model #VE 20ALM.
3. Vishay V/E-25 scan controller model #V1E-25.
4. Vishay V/E-21 switch, balance and calibration module; model #V/E-21AL.
5. Vishay V/E-22 printer, model #V/E-22NB.
6. Pressure gage, dura gage, bronze tube 0-200 psig, calibrated 7-84 by SMD.

Location and Function of Rosettes - (Fig. 1)

- Strain rosette A, B and C - to investigate the adequacy of the column and chimney reinforcement rings.
- Strain rosette D - to investigate the bending stress in the horizontal bar because of the offset created by the vacuum shell halves.
- Strain rosette E and G - to investigate the stresses created due to edge moments.
- Strain rosette F and J - to investigate the bending stresses in the shell due to the offset created by the vacuum shell halves.
- Strain rosette H and I - to investigate the stresses in the vacuum shell far away from any rigid supports.

TEST PROCEDURE:

1. Verify that all the equipment and gages are plumbed and wired correctly, Fig. 1 and Fig. 2 respectively. Before initiating pressure test exclude all nonessential personnel from the Muon Hall experimental floor. Also go through the check list given below.

CHECK LIST

CHIMNEY AREA:

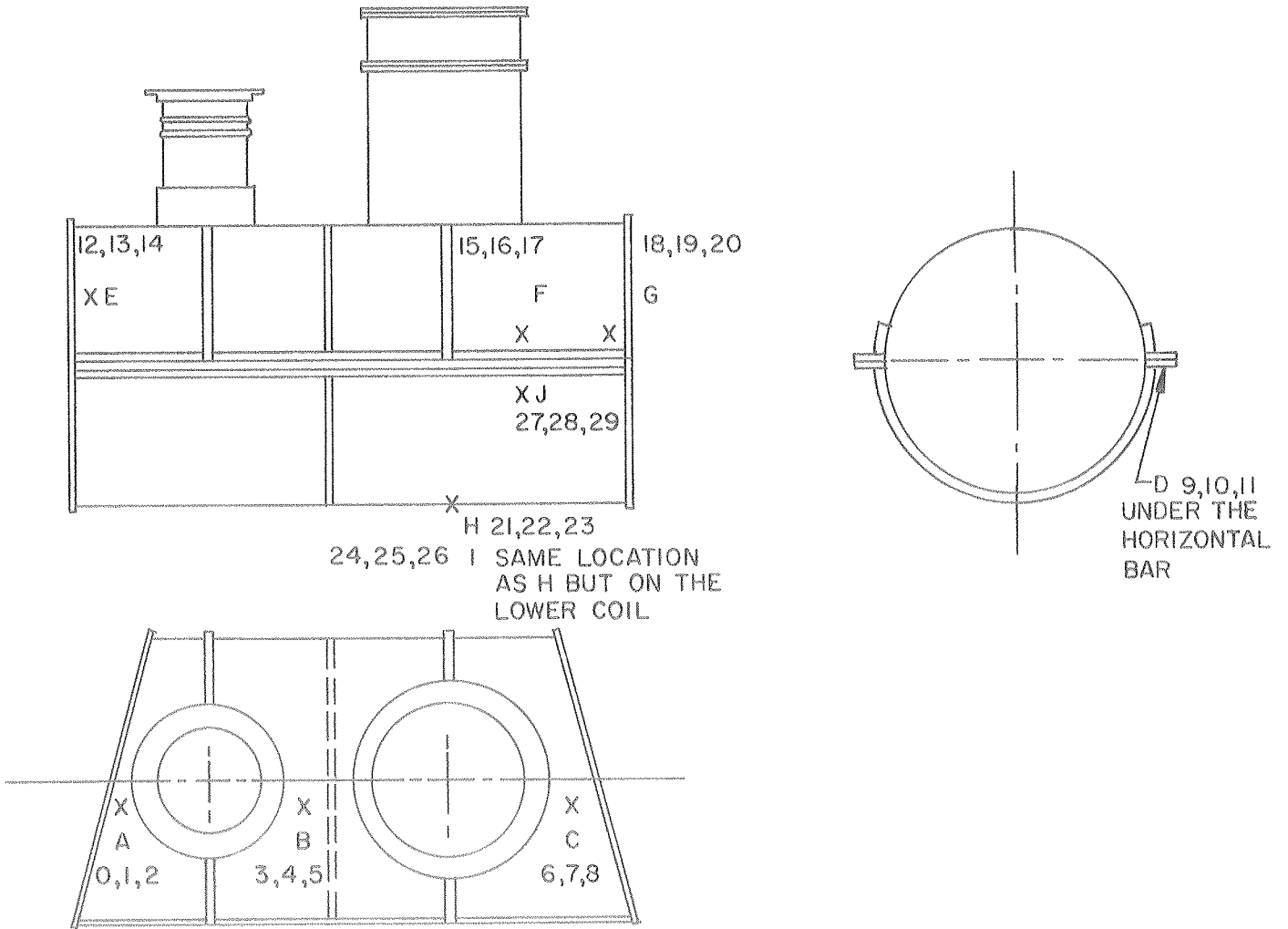
1. Fill line plugged and restrained.
2. Vent line plugged and restrained.
3. Top hat vent line plugged.
4. Small feed through plugged and restrained.
5. Valve on pressure gage closed.
6. Current lead flow holes are plugged and restrained.
7. Both helium vents on chimney plugged and restrained.
8. Restrain liquid level probes.
9. Close bellows type vacuum valve.
10. Make sure the guts are taken out of the pump out port.

UPPER COIL:

1. Coil position indicators restrained.
2. Check to see that the nitrogen inlet is sealed and restrained.

LOWER COIL:

1. Make sure that the pump out port is sealed.
2. Coil position indicators are restrained.
3. Close bellows type vacuum valve.
4. Check to see the 4-inch vacuum rupture disk is sealed and secured.



NOTE: Strain rosette A has a g.F. of 2.03, all the other strain rosettes have a g.F. of 2.01

Fig. 1. Strain Rosettes Locations for CCM Vacuum Jacket Pressure Test

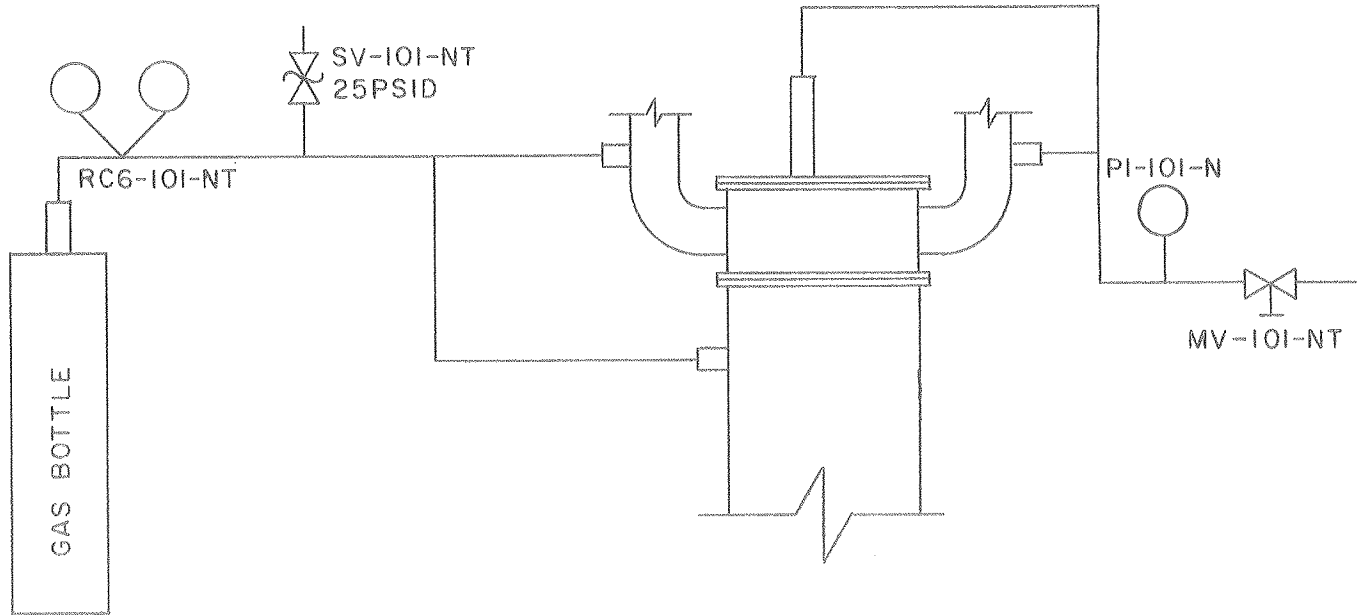


Fig. 2. Flow Schematic for the CCM Vacuum Jacket Pressure Test

2. Balance and calibrate the strain gages.
3. Gradually increase the internal pressure to 12 psid.
4. Determine the highest stress intensity on the vacuum jacket by reducing the strain readings graphically from the strain rosette into stress intensity at this location. Double this stress intensity and check to see if it is less than $(12 \times 10^3)(1.5) = 18 \times 10^3$ psi, if true then continue with the pressure test, if not true stop the test.
5. Gradually increase the internal pressure in ~3 psid increments until the test pressure is achieved. Hold each pressure increment for 10 minutes and record the microstrain and internal calibration of each strain gage. Actual test pressures and holding times given in Appendix A.
6. Hold the vacuum jacket at the prescribed test pressure of 24 psid for ten minutes.
7. Reduce pressure to 12 psid, record the microstrain and internal calibration of each strain gage. Leak check feed throughs.
8. Decrease pressure to 0 psid and record the microstrain and internal calibration of each strain gage.

CALCULATIONS - REDUCTION OF RESULTS:

There are two methods; graphical and analytical that may be used to reduce the rosette data. A description of both methods is given below.

Graphical method

A graphical vector solution was used to determine the stress intensity at the location of maximum strain during the test at the first pressure increment (12 psid). This method is described in "The Handbook of Experimental Stress Analysis" by M. Hetenyi.

To use the graphical method several parameters must be determined initially. First a stress scale must be chosen - (1000 psi per inch). Next the scale that is used along the abscissa to find the center of Mohr's circle must be determined as follows

$$[\text{stress scale}] \times \frac{3(1 - \mu)}{E}$$

μ = Poisson's ratio = 0.305

E = Young's modulus = 27.6×10^6 psi

∴ the abscissa scale to find the center of Mohr's circle

$$= \frac{(1000) (3) (1 - 0.305)}{27.6 \times 10^6}$$

$$= 75.6 \text{ microstrain/inch of graph}$$

The scale that is used to find the radius of Mohr's circle must be determined as follows. Since there are two different types of strain rosettes used, this calculation must be done twice.

$$[\text{stress scale}] \frac{(3) (1 + \mu)}{2 E} + \frac{1 - K}{1 + K}$$

$$K = \frac{3}{2b-1}$$

b = manufacturers auxiliary sensitivity coefficient

$b_1 = -200$ for strain rosette A only

$b_2 = +156$ for all the strain rosettes except for strain rosette A

$$\therefore K_1 = -7.48 \times 10^{-3}$$

$$\therefore K_2 = +9.65 \times 10^{-3}$$

\therefore the scale 1 to find the radius of Mohr's circle

$$= (1000) \frac{(3) (1 + 0.305)}{2 (27.6 \times 10^6)} \frac{1 - (-7.48 \times 10^{-3})}{1 - 7.48 \times 10^{-3}}$$

$$= 72.0 \text{ microstrain/inch of graph}$$

\therefore the scale 2 to find the radius of Mohr's circle

$$= (1000) \frac{(3) (1 + 0.305)}{2 (27.6 \times 10^6)} \frac{1 - 9.65 \times 10^{-3}}{1 + 9.65 \times 10^{-3}}$$

$$= 69.6 \text{ microstrain/inch of graph.}$$

Figure 3 shows how this graphical method is applied using the following strain values.

$$\epsilon_1 = 115 \text{ microstrain}$$

$$\epsilon_2 = 71 \text{ microstrain}$$

$$\epsilon_3 = 51 \text{ microstrain}$$

These are the strain values
from rosette (I).
Where $\epsilon_1 > \epsilon_2 > \epsilon_3$

STRAIN VS. STRESS AT 12.0 PSID
 THE THIRD PRINCIPLE STRESS IS
 THE INTERNAL PRESSURE OF 120 PSID.
 DATE: 7/23/85
 BY: ROMAN DACHNINSKY

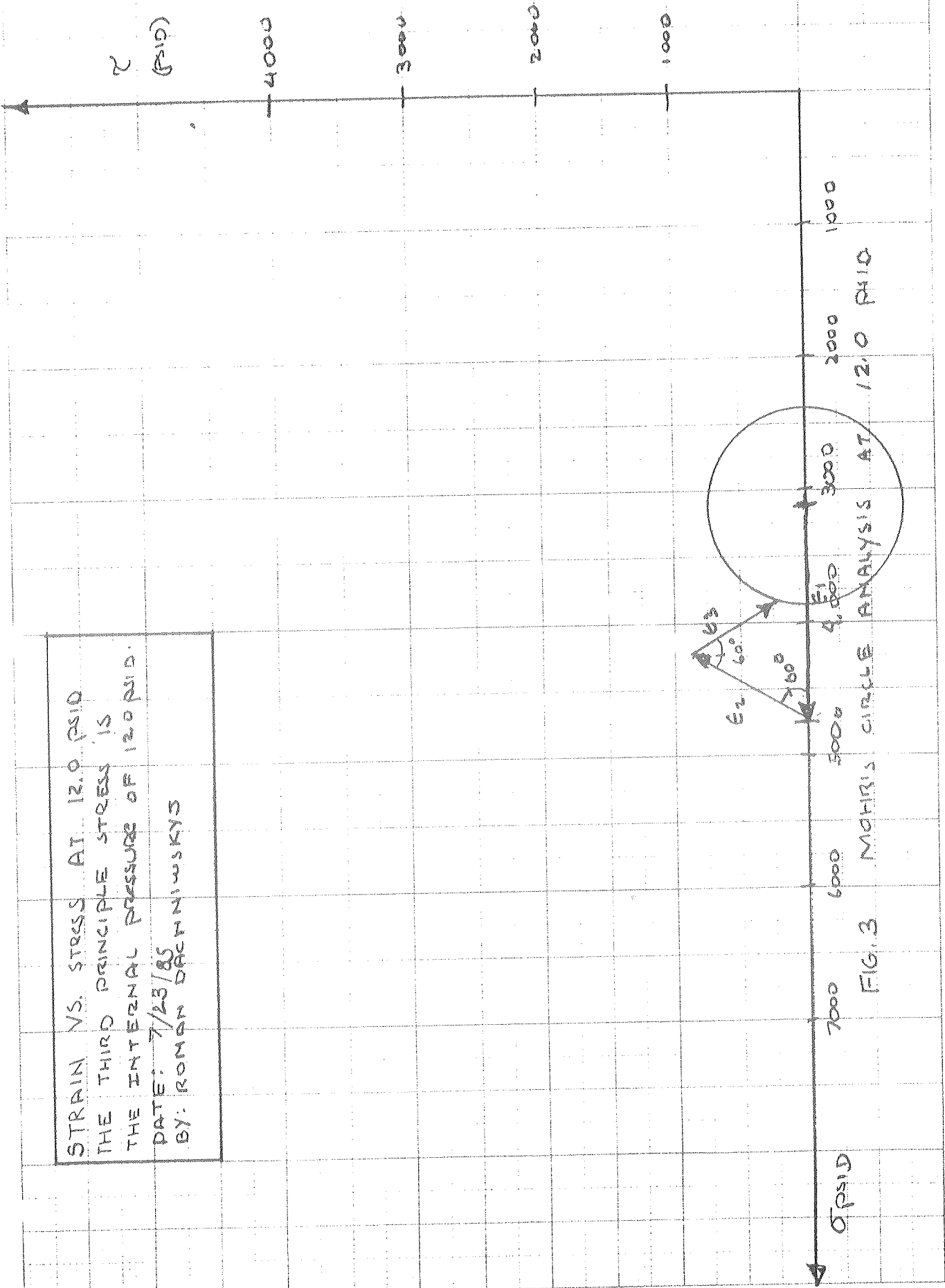


FIG. 3 MOHR'S CIRCLE ANALYSIS AT 12.0 PSID

To find the center of Mohr's circle, one must place a point on the abscissa the number of inches shown below away from the origin.

$$\frac{\epsilon_1 + \epsilon_2 + \epsilon_3}{75.6} = 3.13 \text{ inches}$$

To find the radius of Mohr's circle, one must determine the length of the following three vectors as shown below:

$$\vec{\epsilon}_1 = \frac{115}{69.6} = 1.64 \text{ in}$$

$$\vec{\epsilon}_2 = \frac{71}{69.6} = 1.02 \text{ in}$$

$$\vec{\epsilon}_3 = \frac{51}{69.6} = 0.73 \text{ in}$$

The placement of these vectors is shown in Fig. 3.

To determine the stress intensity being measured by this strain rosette, one must draw a circle having its center as defined above and its radius defined by the end of vector $\vec{\epsilon}_3$.

The principal stresses given by this Mohr's circle are 3,850 psi and -2400 psi. The third principal stress is the internal test pressure of 12 psid.

$$\therefore \sigma_1 = 3,850 \text{ psi} \quad \text{where } \sigma_1 > \sigma_2 > \sigma_3$$

$$\sigma_2 = 2,400 \text{ psi}$$

$$\sigma_3 = 12 \text{ psi}$$

$$\begin{aligned} \text{The stress intensity} &= \sigma_1 - \sigma_3 \\ &= 3,838 \text{ psi} \end{aligned}$$

Analytical Method

The strains recorded from the strain rosettes can also be reduced to principal stresses using the following analytical method. This method will be shown below as a sample calculation using the same strains as given in the graphical method. This method is also described in M. Hetenyi's book.

$$\therefore \epsilon_1 = 115 \text{ microstrain}$$

$$\epsilon_2 = 71 \text{ microstrain}$$

$$\epsilon_3 = 51 \text{ microstrain}$$

The following parameters must be initially calculated.

$$A = 1/3 (\epsilon_1 + \epsilon_2 + \epsilon_3)$$

$$B = \sqrt{2}/3 [(\epsilon_1 - \epsilon_2)^2 + (\epsilon_2 - \epsilon_3)^2 + (\epsilon_1 - \epsilon_3)^2]^{1/2}$$

$$\therefore A = 79.0 \text{ microstrain}$$

$$\therefore B = 37.8 \text{ microstrain}$$

Next it is necessary to correct for the transverse gage sensitivity in B.

$$B' = B \frac{(1 + K)}{(1 - K)}$$

$$K = \frac{3}{2b-1} = 9.65 \times 10^{-3}$$

$$\therefore B' = 38.5 \text{ microstrain}$$

Next the components that make up the principal stresses are determined:

$$A'' = \frac{A E}{1 - \mu}$$

$$E = \text{Young's modulus} = 27.6 \times 10^6 \text{ psi}$$

$$\mu = \text{Poisson's ratio} = 0.305$$

$$B'' = \frac{B' E}{1 + \mu}$$

$$\therefore = 3,137 \text{ psi}$$

$$\therefore = 814 \text{ psi}$$

Determining the principal stresses

$$\sigma_{\max} = A'' + B''$$

$$= 3,137 + 814 = 3,951 \text{ psi}$$

$$\sigma_{\min} = A'' - B''$$

$$= 3,137 - 814 = 2,323 \text{ psi}$$

The third principal stress is the internal pressure of 12 psi

$$\begin{aligned} \sigma_1 &= 3,951 \text{ psi} && \text{where } \sigma_1 > \sigma_2 > \sigma_3 \\ \sigma_2 &= 2,323 \text{ psi} \\ \sigma_3 &= 12 \text{ psi} \end{aligned}$$

$$\begin{aligned} \text{The stress intensity} &= \sigma_1 - \sigma_3 \\ &= 3,951 - 12 \\ &= 3,939 \text{ psi} \end{aligned}$$

REDUCTION OF THE STRAIN ROSETTE DATA

Table I contains all the data that was recorded during the pressure test. Table II contains all the stress intensity values experienced by all the strain rosettes when the vacuum jacket was at 24 psid.

DISCUSSION OF THE STRAIN ROSETTE RESULTS AND DATA

Table III shows that the increase in strain registered by the strain rosettes was linearly proportional to the increase in test pressure. This demonstrates that the area being instrumented was not yielding. Table II shows that the highest stress intensity experienced by the vacuum shell during the pressure test was 7,881 psi. This is far below the allowable stress intensity per ASME code and FSM 14.1 of $[(18.8 \times 10^3)(0.8)(1.5)](0.8) = 18.0 \times 10^3$ psi. This information indicates that the vacuum shell could have been pressurized to

$$\frac{18.0 \times 10^3}{7.88 \times 10^3} (24) = 54.8 \text{ psi}$$

assuming that the welds are adequate. None of the strain gauges showed an appreciable amount of permanent set when the test pressure was reduced. This can be verified by comparing the strain readings of data sheet number one with data sheet number eight. The readings should be same if there is no permanent set.

CONCLUSION

The CCM vacuum jacket showed no unusual signs during the pressure test. The stress intensities at 24 psi are below the allowable, therefore the CCM vacuum jacket will safely withstand the expected maximum pressure of 16 psi if the helium reservoir should rupture.

Table I
Strain Rosette Results

Data Sheet #1

Pressure = 0 psig (initial readings)

Strain Gage Channel Numbers	Microstrain (10^{-6} in/in)
A — 00	001
— 01	001
— 02	000
B — 03	001
— 04	001
— 05	001
C — 06	001
— 07	000
— 08	001
D — 09	000
— 10	000
— 11	000
E — 12	000
— 13	000
— 14	000
F — 15	000
— 16	000
— 17	001
G — 18	000
— 19	001
— 20	000
H — 21	000
— 22	001
— 23	001
I — 24	000
— 25	000
— 26	000
J — 27	000
— 28	001
— 29	001

Data Sheet #2

Pressure = 12.0 psid

Strain Gage Channel Numbers	Microstrain (10^{-6} in/in)
00	016
01	030
02	009
03	059
04	019
05	068
06	017
07	040
08	041
09	030
10	029
11	029
12	010
13	029
14	005
15	056
16	010
17	015
18	039
19	035
20	007
21	023
22	055
23	017
24	051
25	071
26	115
27	047
28	079
29	049

Table I (cont.)

Data Sheet #3

Pressure = 14 psid

Strain Gage Channel Number	Microstrain (10^{-6} in/in)
00	020
01	040
02	013
03	075
04	026
05	086
06	021
07	052
08	053
09	037
10	021
11	036
12	013
13	038
14	006
15	072
16	013
17	020
18	051
19	045
20	008
21	030
22	070
23	020
24	063
25	089
26	144
27	061
28	102
29	061

Data Sheet #4

Pressure = 17.0 psid

Strain Gage Channel Number	Microstrain (10^{-6} in/in)
00	023
01	046
02	014
03	083
04	028
05	096
06	023
07	061
08	061
09	042
10	024
11	040
12	014
13	043
14	006
15	081
16	016
17	023
18	057
19	051
20	008
21	035
22	079
23	023
24	073
25	100
26	161
27	069
28	116
29	069

Table I (cont.)

Data Sheet #5

Pressure = 20.0 psid

Strain Gage Channel Number	Microstrain (10^{-6} in/in)
00	027
01	053
02	016
03	097
04	034
05	114
06	027
07	073
08	073
09	050
10	029
11	047
12	016
13	055
14	007
15	097
16	019
17	029
18	069
19	061
20	009
21	042
22	093
23	027
24	086
25	119
26	189
27	082
28	140
29	083

Data Sheet #6

Pressure = 24 psid

Strain Gage Channel Number	Microstrain (10^{-6} in/in)
00	068
01	019
02	019
03	115
04	043
05	141
06	034
07	089
08	065
09	061
10	037
11	058
12	019
13	071
14	007
15	120
16	120
17	038
18	084
19	077
20	012
21	051
22	113
23	032
24	105
25	145
26	227
27	102
28	176
29	103

Table I (cont.)

Data Sheet #7

Pressure = 12 psid (depressuring)

Strain Gage Channel Number	Microstrain (10^{-6} in/in)
00	017
01	039
02	012
03	(?)
04	025
05	081
06	020
07	049
08	050
09	037
10	021
11	035
12	013
13	038
14	006
15	068
16	012
17	021
18	047
19	044
20	007
21	029
22	067
23	019
24	061
25	085
26	137
27	058
28	100
29	060

Data Sheet #8

Pressure = 0 psig (final readings)

Strain Gage Channel Number	Microstrain (10^{-6} in/in)
00	003
01	000
02	001
03	004
04	001
05	002
06	001
07	000
08	001
09	001
10	001
11	000
12	002
13	001
14	002
15	001
16	001
17	001
18	001
19	002
20	000
21	001
22	001
23	001
24	001
25	000
26	000
27	001
28	003
29	002

Table II
 Stress Intensities at 24 psid: Analytical Method

Strain Rosette	σ_1 (psi)	σ_2 (psi)	σ_3 (psi)	Stress Intensity (psi)
A	1926	24	- 462	2388
B	5260	2740	24	5236
C	3522	1998	24	3498
D	2096	0	-1032	3128
E	2134	450	24	2110
F	3597	24	- 3	3581
G	2907	1173	24	2883
H	3663	1561	24	3639
I	7905	4815	24	7881
J	6131	4029	24	6107

Table III
 Comparison of Strains at a Test Pressure
 of 12 psid and 24 psid

Strain Gage Channel	(A) Strain at 12 psid (in/in)	(B) Strain at 24 psid (in/in)	B/A
0	-16	-32	2.0
1	30	68	2.27
2	9	19	2.11
3	59	115	1.95
4	19	43	2.26
5	58	141	2.07
6	17	34	2.00
7	40	89	2.23
8	41	85	2.07
9	30	61	2.03
10	17	37	2.18
11	-29	-58	2.0
12	10	19	1.90
13	29	71	2.45
14	5	7	1.4
15	56	120	2.14
16	-10	-24	2.40
17	15	38	2.53
18	39	64	1.64
19	35	77	2.20
20	7	12	1.71
21	23	51	2.22
22	55	113	2.05
23	17	32	1.88
24	51	105	2.06
25	71	143	2.01
26	115	227	1.97
27	47	102	2.17
28	79	176	2.23
29	49	103	2.10

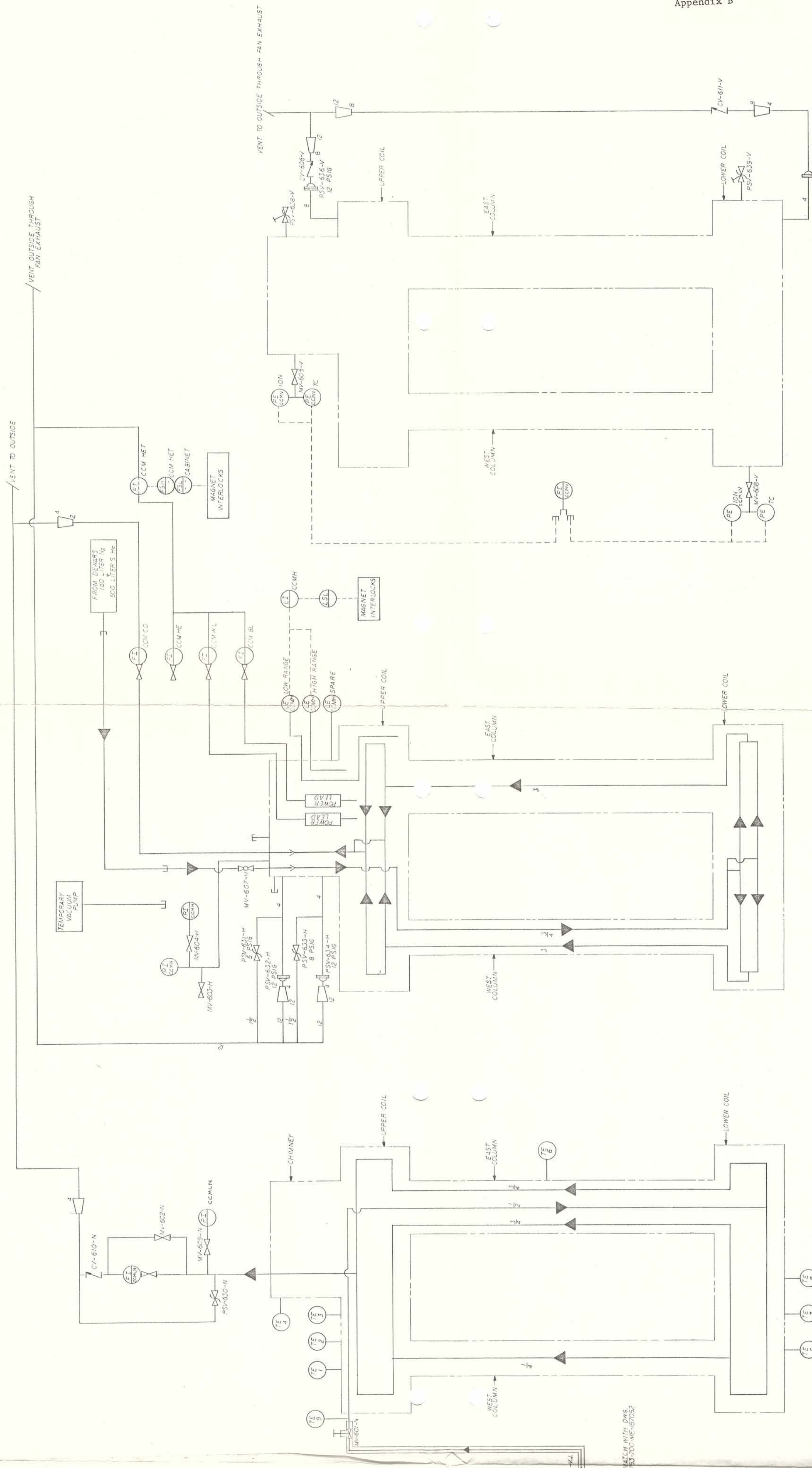
Appendix A: Pressure Test Data Sheet

Date: 7/24/85

Test	Pressure	Time (start ; finish)	Initials of Operator
0	psid	5:48 a.m.	RD
12		6:28 ; 6:31	RD
14		6:43 ; 6:45	RIP
17		6:50 ; 6:55	RD
20		7:03 ; 7:06	RD
24		7:15 ; 7:25	RD
0		10:00 ;	RD

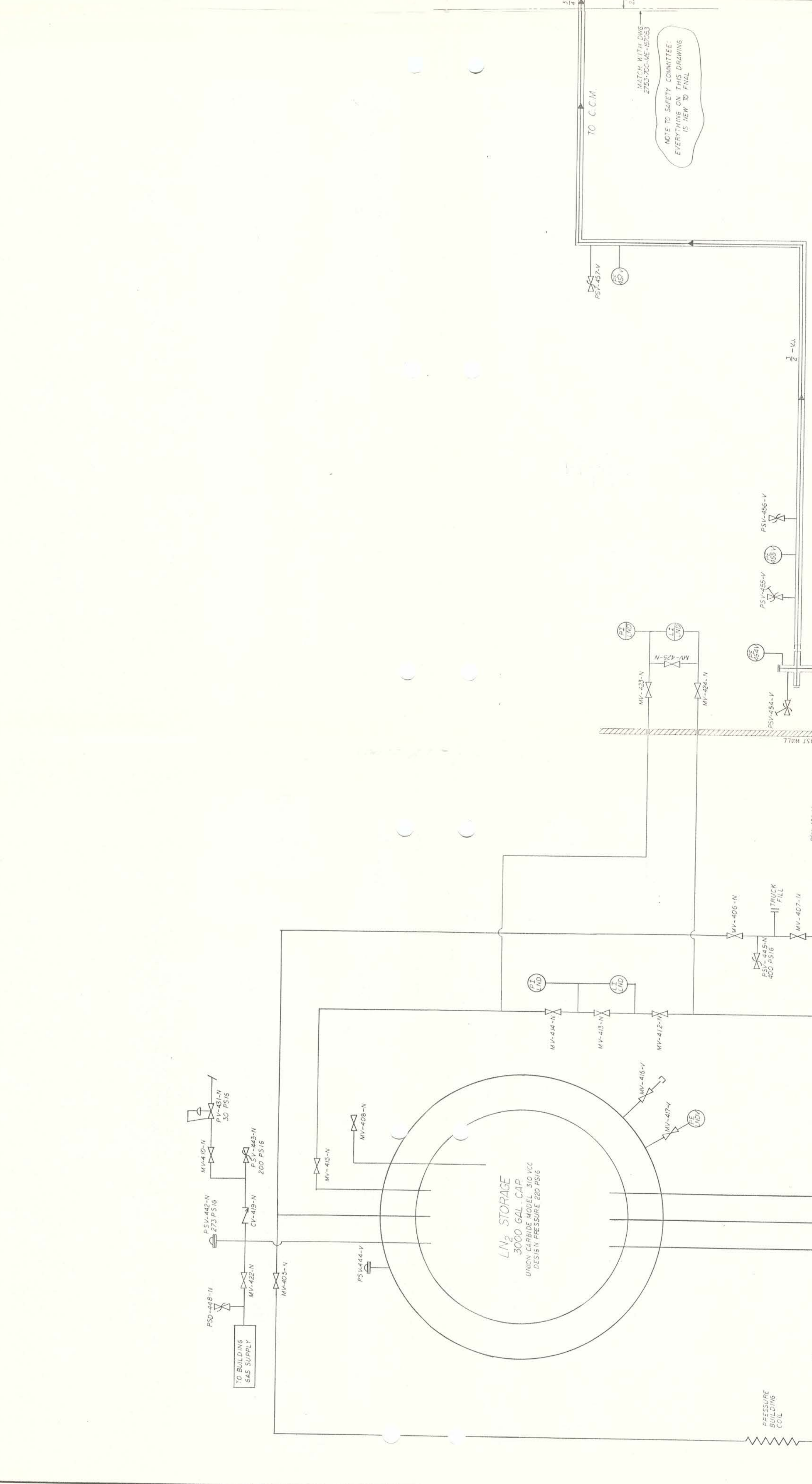
Comment: Pressure held steadily at 24 psid.

JUL 12 1985



REV.	DATE	DESCRIPTION
1		
2		
3		
4		
5		
6		
7		
8		
9		
10		
11		
12		
13		
14		
15		
16		
17		
18		
19		
20		
21		
22		
23		
24		
25		
26		
27		
28		
29		
30		
31		
32		
33		
34		
35		
36		
37		
38		
39		
40		
41		
42		
43		
44		
45		
46		
47		
48		
49		
50		
51		
52		
53		
54		
55		
56		
57		
58		
59		
60		
61		
62		
63		
64		
65		
66		
67		
68		
69		
70		
71		
72		
73		
74		
75		
76		
77		
78		
79		
80		
81		
82		
83		
84		
85		
86		
87		
88		
89		
90		
91		
92		
93		
94		
95		
96		
97		
98		
99		
100		

JUL 12 1985



REV.	DATE	DESCRIPTION
1		
2		
3		
4		
5		
6		
7		
8		
9		
10		
11		
12		
13		
14		
15		
16		
17		
18		
19		
20		
21		
22		
23		
24		
25		
26		
27		
28		
29		
30		
31		
32		
33		
34		
35		
36		
37		
38		
39		
40		
41		
42		
43		
44		
45		
46		
47		
48		
49		
50		
51		
52		
53		
54		
55		
56		
57		
58		
59		
60		
61		
62		
63		
64		
65		
66		
67		
68		
69		
70		
71		
72		
73		
74		
75		
76		
77		
78		
79		
80		
81		
82		
83		
84		
85		
86		
87		
88		
89		
90		
91		
92		
93		
94		
95		
96		
97		
98		
99		
100		

NOTE TO SAFETY COMMITTEE: EVERYTHING ON THIS DRAWING IS NEW TO PHIL.

DESIGN WITH PMS 2703, MC-57052

FERMI NATIONAL ACCELERATOR LABORATORY UNITED STATES DEPARTMENT OF ENERGY

CRYOGENICS MUON LAB LN₂ STORAGE SYSTEM SCHEMATIC

SCALE: DRAWING NUMBER: 27-53-900-ME-167C.02

SCALE: DRAWING NUMBER: 27-53-900-ME-167C.03

SCALE: DRAWING NUMBER: 27-53-900-ME-167C.04

SCALE: DRAWING NUMBER: 27-53-900-ME-167C.05

SCALE: DRAWING NUMBER: 27-53-900-ME-167C.06

SCALE: DRAWING NUMBER: 27-53-900-ME-167C.07

SCALE: DRAWING NUMBER: 27-53-900-ME-167C.08

SCALE: DRAWING NUMBER: 27-53-900-ME-167C.09

SCALE: DRAWING NUMBER: 27-53-900-ME-167C.10

SCALE: DRAWING NUMBER: 27-53-900-ME-167C.11

SCALE: DRAWING NUMBER: 27-53-900-ME-167C.12

SCALE: DRAWING NUMBER: 27-53-900-ME-167C.13

SCALE: DRAWING NUMBER: 27-53-900-ME-167C.14

SCALE: DRAWING NUMBER: 27-53-900-ME-167C.15

SCALE: DRAWING NUMBER: 27-53-900-ME-167C.16

SCALE: DRAWING NUMBER: 27-53-900-ME-167C.17

SCALE: DRAWING NUMBER: 27-53-900-ME-167C.18

SCALE: DRAWING NUMBER: 27-53-900-ME-167C.19

SCALE: DRAWING NUMBER: 27-53-900-ME-167C.20

SCALE: DRAWING NUMBER: 27-53-900-ME-167C.21

SCALE: DRAWING NUMBER: 27-53-900-ME-167C.22

SCALE: DRAWING NUMBER: 27-53-900-ME-167C.23

SCALE: DRAWING NUMBER: 27-53-900-ME-167C.24

SCALE: DRAWING NUMBER: 27-53-900-ME-167C.25

SCALE: DRAWING NUMBER: 27-53-900-ME-167C.26

SCALE: DRAWING NUMBER: 27-53-900-ME-167C.27

SCALE: DRAWING NUMBER: 27-53-900-ME-167C.28

SCALE: DRAWING NUMBER: 27-53-900-ME-167C.29

SCALE: DRAWING NUMBER: 27-53-900-ME-167C.30

SCALE: DRAWING NUMBER: 27-53-900-ME-167C.31

SCALE: DRAWING NUMBER: 27-53-900-ME-167C.32

SCALE: DRAWING NUMBER: 27-53-900-ME-167C.33

SCALE: DRAWING NUMBER: 27-53-900-ME-167C.34

SCALE: DRAWING NUMBER: 27-53-900-ME-167C.35